



Utility-Scale Parabolic Trough Solar Systems: Performance Acceptance Test Guidelines

April 2009 — December 2010

David Kearney
Kearney & Associates
Vashon, Washington



NREL is a national laboratory of the U.S. Department of Energy, Office of Energy Efficiency & Renewable Energy, operated by the Alliance for Sustainable Energy, LLC.

Subcontract Report
NREL/SR-5500-48895
May 2011

Contract No. DE-AC36-08GO28308

Utility-Scale Parabolic Trough Solar Systems: Performance Acceptance Test Guidelines

April 2009 — December 2010

David Kearney
Kearney & Associates
Vashon, Washington

NREL Technical Monitor: Mark Mehos
Prepared under Subcontract No. AXL-9-99218-01

NREL is a national laboratory of the U.S. Department of Energy, Office of Energy Efficiency & Renewable Energy, operated by the Alliance for Sustainable Energy, LLC.

NOTICE

This report was prepared as an account of work sponsored by an agency of the United States government. Neither the United States government nor any agency thereof, nor any of their employees, makes any warranty, express or implied, or assumes any legal liability or responsibility for the accuracy, completeness, or usefulness of any information, apparatus, product, or process disclosed, or represents that its use would not infringe privately owned rights. Reference herein to any specific commercial product, process, or service by trade name, trademark, manufacturer, or otherwise does not necessarily constitute or imply its endorsement, recommendation, or favoring by the United States government or any agency thereof. The views and opinions of authors expressed herein do not necessarily state or reflect those of the United States government or any agency thereof.

Available electronically at <http://www.osti.gov/bridge>

Available for a processing fee to U.S. Department of Energy and its contractors, in paper, from:

U.S. Department of Energy
Office of Scientific and Technical Information

P.O. Box 62
Oak Ridge, TN 37831-0062
phone: 865.576.8401
fax: 865.576.5728
email: <mailto:reports@adonis.osti.gov>

Available for sale to the public, in paper, from:

U.S. Department of Commerce
National Technical Information Service
5285 Port Royal Road
Springfield, VA 22161
phone: 800.553.6847
fax: 703.605.6900
email: orders@ntis.fedworld.gov
online ordering: <http://www.ntis.gov/help/ordermethods.aspx>

Cover Photos: (left to right) PIX 16416, PIX 17423, PIX 16560, PIX 17613, PIX 17436, PIX 17721, PIX 18201 (used with permission of Acciona Solar Power)



Printed on paper containing at least 50% wastepaper, including 10% post consumer waste.

Acknowledgements

This report has benefited considerably during its development by careful and frequent scrutiny from an active and experienced Advisory Committee and from critique by many stakeholders in the final review cycles. Throughout this process, the guidance, contributions and co-authorship of NREL Concentrating Solar Power Program Manager Mark Mehos have strengthened and honed the end product. Through his additional responsibility as Operating Agent of the SolarPACES Task 1 Committee on System Analysis, which is also partially focused on acceptance testing, members of that task group also participated in the review cycle. We sincerely thank all of the above reviewers for their time and effort.

The Advisory Committee and several others deserve special mention for their many contributions during this project and travel to NREL for periodic meetings. They are Gary Aron and Ryan Bowers (Worley Parsons), Geoff Baxter (NextLight), Georg Brakmann and Mathias Wiemann (Fichtner Solar), Gilbert Cohen (Eliosol), Jim Doubek and Todd Eagleston (NV Energy), Ray Dracker and Jake McKee (Solar Millennium), Ronald Flood and Phil Smithers (APS), Michael Henderson (R.W. Beck), Ulf Herrmann (Flagsol), Chris Jensen and Marcus Weber (Fluor Power), Chuck Kutscher (NREL), Hank Price and Bruce Kelly (Abengoa Solar), and Kurt Westermann (Black & Veatch). The work of Mike Wagner (NREL) on modeling of equilibrium effects in the solar system has been of particular value. Finally, the excellent support of Teri Spinuzzi of NREL is gratefully acknowledged.

David Kearney
Kearney & Associates

Preface

The purpose of these Guidelines is to provide recommendations for acceptance test guidance for large trough solar systems that can yield results of a high level of accuracy consistent with good engineering knowledge and practice. The recommendations have been developed under a National Renewable Energy Laboratory (NREL) subcontract and reviewed by stakeholders representing concerned organizations and interests throughout the concentrating solar power (CSP) community. These Guidelines recommend certain methods, instrumentation, equipment operating requirements, and calculation methods. When tests are run in accordance with these Guidelines, we expect that the test results will yield a valid indication of the actual performance of the tested equipment. But these are only recommendations—to be carefully considered by the contractual parties involved in the acceptance tests—and we expect that modifications may be required to fit the particular characteristics of a specific project.

These Guidelines do not specify means to compare test results to contractual guarantees. Therefore, we expect that the parties to a commercial test will address that issue and agree before starting the test and signing the contract on the method to be used for evaluating the test results. The approach taken in these Guidelines is that the measured test results will be compared to projections from a performance model based on the measured meteorological conditions and agreed-upon solar system characteristics.

The scope of the solar system discussed in these Guidelines does not include a thermal energy storage (TES) system. But even if the scope did include a TES system, the methods of testing the solar field/heat transfer fluid system itself would be similar, if not identical, to the guidance given in this document. A separate set of tests and objectives would be required for TES system acceptance.

A recently formed American Society of Mechanical Engineers (ASME) committee is working on *Performance Test Code¹ 52 – Concentrating Solar Power Plants* that should supplant this Guideline within several years. This work will be provided to that committee as a reference for its deliberations.

¹ Often abbreviated as PTC.

Definitions and Description of Terms

For further reference, ASME *PTC 2 – Definitions and Values* contains definitions of terms and values of physical constants and conversion factors common to equipment testing and analysis.

Definitions

- **acceptance test:** The evaluating action(s) to determine if a new or modified piece of equipment satisfactorily meets its performance criteria, permitting the purchaser to "accept" it from the supplier.
- **accuracy:** The closeness of agreement between a measured value and the true value.
- **aperture area:** The projection on the aperture plane of the active mirror collecting area of a parabolic trough, i.e., projection of the reflective surface less gaps between the mirror panels.
- **aperture of parabolic trough:** The width between the reflector edges on a plane across the aperture of a parabolic reflector (the aperture plane).
- **base reference conditions:** The values of all the external parameters, i.e., parameters outside the test boundary to which the test results are corrected.
- **bias error:** See *systematic error*.
- **calibration:** The process of comparing the response of an instrument to a standard instrument over some measurement range and adjusting the instrument to match the standard if appropriate.
- **incidence angle (θ):** The angle between a direct ray from the sun and the aperture plane of the parabolic trough collector (defined to be 0 degrees when the rays are normal to the aperture plane). The effect of incidence angle on performance is contained in the **incidence angle modifier**, or **IAM**.
- **influence coefficient:** See *sensitivity*: the ratio of the change in a result to a unit change in a parameter.
- **instrument:** A tool or device used to measure physical dimensions of length, thickness, width, weight, or any other value of a variable. These variables can include: size, weight, pressure, temperature, fluid flow, voltage, electric current, density, viscosity, and power. Sensors are included that may not, by themselves, incorporate a display but transmit signals to remote computer-type devices for display, processing, or process control. Also included are items of ancillary equipment directly affecting the display of the primary instrument, e.g., an ammeter shunt. Also included are tools or fixtures used as the basis for determining part acceptability.
- **measurement error (δ):** The true, unknown difference between the measured value and the true value.
- **parties to a test:** Those persons and companies contractually interested in the results.
- **precision error:** See *random error*.
- **primary variables:** Those variables used in calculations of test results. Further classified as:
 - Class 1: primary variables have a relative influence coefficient of 0.2 or greater

- Class 2: primary variables have a relative influence coefficient of less than 0.2
- Refer to *PTC 19.1 - Test Uncertainty* for the determination of relative sensitivity coefficients.

- **random error (ϵ):** Sometimes called precision; the true random error, which characterizes a member of a set of measurements. ϵ varies in a random, Gaussian-normal manner from measurement to measurement.
- **random uncertainty:** Estimate of \pm limits of random error within a defined level of confidence. Often given for $2\text{-}\sigma$ (2 standard deviations) confidence level of about 95%.
- **rated solar thermal design power (or capacity):** The level of solar thermal output power from the solar system that will drive the turbine cycle at design electrical load.
- **secondary variables:** Variables that are measured but do not enter into the calculation.
- **sensitivity:** See *influence coefficient*; the ratio of the change in a result to a unit change in a parameter.
- **serialize:** Means that an instrument has been assigned a unique number and that number has been permanently inscribed on or to the instrument so that it can be identified and tracked.
- **soiling factor:** A factor that describes the dirtiness, or soiling, of the reflective surface (e.g., glass mirrors or silvered film) of the parabolic trough collectors; specifically, at any given time, the actual reflectivity normalized by the design or as-new reflectivity.
- **solar multiple:** Equals [(solar field aperture area) / (solar field aperture area sufficient to deliver the design solar thermal output power at stated conditions of DNI and incident angle, e.g., 950 W/m^2 at 0 degrees incidence angle)].
- **solar system thermal efficiency:** Ratio of the solar thermal power output of the solar system normalized by the product of the incident direct beam radiation and the total aperture area of the solar field. See Equation (Eqn.) 3-2.
- **systematic error (β):** Sometimes called bias; the true systematic or fixed error, which characterizes every member of any set of measurements from the population. It is the constant component of the total measurement error (δ).
- **systematic uncertainty (**B**):** An estimate of the \pm limits of systematic error with a defined level of confidence (usually 95%).
- **test boundary:** Identifies the energy streams required to calculate corrected results.
- **test reading:** One recording of all required test instrumentation.
- **test run:** A group of test readings that satisfy the stated criteria for test conditions, e.g., with regard to thermally stability.
- **traceable:** Records are available demonstrating that the instrument can be traced through a series of calibrations to an appropriate ultimate reference such as National Institute for Standards and Technology (NIST).
- **ullage:** The unfilled space in a container of liquid.

- **uncertainty (U):** $\pm U$ is the interval about the measurement or result that likely contains the true value for a certain level of confidence.

Abbreviations and Acronyms

| | |
|------|---|
| ANI | aperture normal insolation (DNI vector normal to aperture plane) |
| COD | commercial operation date |
| CSP | concentrating solar power |
| DSC | digital scanning calorimetry |
| DHI | diffuse horizontal irradiance |
| DNI | direct normal insolation (direct [beam] solar radiation on plane normal to sun's ray) |
| EPC | engineering, procurement, and construction contractor |
| Eqn. | equation |
| GHI | global horizontal irradiance |
| HCE | heat collection element or receiver tube or receiver |
| HTF | heat transfer fluid |
| HX | heat exchanger |
| IAM | incidence angle modifier – optical characteristic affecting performance |
| IPP | independent power producer |
| KJOC | Kramer Junction Operating Company |
| L/D | length/diameter ratio |
| LOC | local controller |
| MOV | motor-operated valves |
| mRad | milliradian – a measure of optical error |
| NREL | National Renewable Energy Laboratory |
| O&M | operations and maintenance |
| OJT | on-the-job training |

PTC performance test code

RSR rotating shadowband radiometer

RTD resistance temperature detectors

SAM System Advisor Model, produced by NREL, Sandia National Labs, and DOE

SCA solar collector assembly

SEGS solar electricity generating systems

SF solar field

SFC solar field control system

SM solar multiple

SRC steam Rankine cycle

STG steam turbine generator set

TC thermocouple

TES thermal energy storage

TP technology provider

Table of Contents

| | |
|--|------------|
| Acknowledgements | iii |
| Preface | iv |
| Definitions and Description of Terms | v |
| Definitions..... | v |
| Abbreviations and Acronyms | vii |
| List of Figures | xi |
| List of Tables | xi |
| Executive Summary | xii |
| 1 Introduction | 1 |
| 1.1 Technology Description..... | 1 |
| 1.2 Need for Guidelines | 4 |
| 2 Objectives and Scope | 5 |
| 2.1 Parties to the Acceptance Tests..... | 5 |
| 2.2 Example Project Scenario | 5 |
| 2.3 Pass / Fail Criteria | 5 |
| 2.4 Readiness for Acceptance Tests..... | 5 |
| 2.5 Unique Characteristics of Solar System Performance Tests and the Role of a Performance Model..... | 6 |
| 2.6 Utility-Scale Solar System Performance Acceptance Tests | 7 |
| 2.7 Solar System Boundaries | 7 |
| 3 Test Definitions | 9 |
| 3.1 Performance Acceptance Test Guidelines | 9 |
| 3.2 Short-Duration Steady-State Thermal Power Test | 9 |
| 3.2.1 Introduction and Purpose | 9 |
| 3.2.2 Solar Resource and Weather | 9 |
| 3.2.3 Specific Test Objectives | 10 |
| 3.2.4 Calculations..... | 10 |
| 3.2.4.1 Delivered Power Calculation | 10 |
| 3.2.4.2 Efficiency Calculation..... | 11 |
| 3.2.4.3 HTF Solar Field Inlet and Outlet Temperatures..... | 11 |
| 3.2.4.4 HTF Physical Properties..... | 11 |
| 3.3 Multi-Day Continuous Energy Test..... | 12 |
| 3.4 Performance Model Projection and Comparison to Measured Results | 12 |
| 3.5 HTF and Solar System Parasitic Power Consumption | 13 |

| | | |
|----------|---|-----------|
| 4 | Test Methods | 14 |
| 4.1 | Introduction..... | 14 |
| 4.2 | Solar Field Test Conditions | 15 |
| 4.2.1 | Solar Field Area, Thermal Power Output, and Design Capacity | 15 |
| 4.2.2 | Solar Field Reflectivity..... | 15 |
| 4.2.3 | Seasonal Example of Hourly ANI Variations..... | 17 |
| 4.3 | Criteria for Adequate Test Durations and Conditions | 19 |
| 4.4 | Criteria for Valid Test Results | 21 |
| 4.4.1 | Thermal Equilibrium and Stabilized Test Conditions | 21 |
| 4.4.2 | Repeatability | 21 |
| 4.4.3 | Impact of ANI Variation on Trough Transient Behavior | 22 |
| 5 | Instrument Selection | 27 |
| 5.1 | Required Data | 27 |
| 5.2 | Reference Solar Field Configuration and Measurement Conditions | 27 |
| 5.3 | Comments on Instruments and Measurements | 29 |
| 5.4 | Temperature Measurement | 30 |
| 5.5 | Flow Measurement..... | 32 |
| 5.5.1 | Velocity Profile..... | 32 |
| 5.5.2 | Upstream/Downstream Requirements for Length/Diameter Ratio..... | 37 |
| 5.6 | Direct Normal Insolation | 37 |
| 5.6.1 | Components of Solar Radiation..... | 37 |
| 5.6.2 | Measurement Options | 38 |
| 5.7 | HTF Physical Properties | 39 |
| 5.8 | Mirror Reflectivity | 39 |
| 6 | Evaluation of Measurement Uncertainty | 41 |
| 6.1 | Measurement Uncertainty..... | 41 |
| 7 | Comments on Test Procedures and Plan | 47 |
| 7.1 | Test Plan..... | 47 |
| 7.1.1 | Example of Contract Agreements Prior to Formulation of a Test Plan..... | 48 |
| 7.1.2 | Some Elements of a Test Plan | 48 |
| 7.1.3 | Sample Test Report Outline..... | 49 |
| 7.2 | Further Observations..... | 50 |
| 7.2.1 | General..... | 50 |
| 7.2.2 | Summary of Agreements To Be Made Between Test Parties..... | 51 |

List of Figures

| | |
|---|-----|
| Figure ES-1. Schematic of solar system boundary and performance model | xii |
| Figure 1-1. SEGS IV, Kramer Junction, California. (Photo from Luz International Ltd., circa 1990) | 1 |
| Figure 1-2. Trough collector schematic. (Illustration from Flagsol GmbH) | 2 |
| Figure 1-3. Plant operation based on utility load profile showing how TES can be used to better match the CSP plant’s output to utility needs. (Graphs from Abengoa Solar) | 3 |
| Figure 2-1. Trough energy input | 7 |
| Figure 2-2. Schematic of solar system boundary and performance model | 8 |
| Figure 4-1. Patterns from ANI analysis: (a) during June, March, and December for the entire day, (b) for the daytime period between 8 a.m. and 4 p.m., and (c) the percent changes in the ANI over the previous 30 minutes during the daytime period for these three months. Location: Golden, Colorado. (Courtesy of NREL) | 18 |
| Figure 4-2. Schematic representation of HTF system elements. | 20 |
| Figure 4-3. Location of two possible test boundaries for the acceptance testing procedure. | 23 |
| Figure 4-4. Transient response of a steadily increasing ANI (typical December) in a system with ideal mass flow rate control. | 24 |
| Figure 4-5. Transient response of a steadily increasing ANI (typical March) in a system with ideal mass flow rate control. | 25 |
| Figure 5-1. Fully developed velocity profile in a pipe. (Courtesy of NREL) | 33 |
| Figure 5-2. Components of solar radiation. (Courtesy of NREL) | 37 |

List of Tables

| | |
|---|----|
| Table 4-1. Example Stabilization Criteria for Short-Duration Steady State Power Tests of a Utility-Scale Parabolic Trough Solar Field | 19 |
| Table 4-2. Example Conditions for Testing Periods, Durations and Data Points for Short-Duration Steady State Power Tests | 21 |
| Table 4-3. Summary of Results for Several Representative ANI Gradients | 25 |
| Table 5-1. Parameters Required for Determining Thermal Power Output and Efficiency of the Solar System | 28 |
| Table 5-2. Temperature Measurement Devices | 31 |
| Table 5-3. HTF Flow Measurement Devices | 34 |
| Table 5-4. Estimated Direct Normal Sub-Hourly Measurement Uncertainties (Percent) | 38 |
| Table 6-1. Table of Data – Solar Field Power | 45 |
| Table 6-2. Summary of Data – Solar Field Power | 45 |
| Table 6-3. Table of Data – Solar Field Efficiency | 46 |
| Table 6-4. Summary of Data – Solar Field Efficiency | 46 |

Executive Summary

Prior to commercial operation, large solar systems in utility-size power plants need to pass a performance acceptance test conducted by the engineering, procurement, and construction (EPC) contractor or owners. In lieu of the present absence of ASME or other international test codes developed for this purpose, the National Renewable Energy Laboratory has undertaken the development of interim guidelines to provide recommendations for test procedures that can yield results of a high level of accuracy consistent with good engineering knowledge and practice. The Guidelines contained here are specifically written for parabolic trough collector systems with a heat-transport system using a high-temperature synthetic oil, but the basic principles are relevant to other CSP systems. The fundamental differences between acceptance of a solar power plant and a conventional fossil-fired plant are the transient nature of the energy source and the necessity to use a performance projection model in the acceptance process. These factors bring into play the need to establish methods to measure steady-state performance, comparison to performance model results, and the reasons to test, and model, multi-day performance within the scope of the acceptance test procedure. The power block and balance-of-plant are not within the boundaries of this Guideline. The current Guideline is restricted to the solar thermal performance of parabolic trough systems, and has been critiqued by a broad range of stakeholders in concentrating solar power development and technology.

The solar system boundary is defined in this case to be the shutoff valves in the heat transfer fluid (HTF) piping at the inlet and outlet of the solar heat exchanger(s), as shown in Figure ES-1. The solar system comprises the solar field and HTF subsystems. The boundary between these subsystems is defined as the shutoff valves on the interconnection piping for each loop to the cold HTF header and hot HTF header, respectively, in each segment of the solar field. The scope of these Guidelines does not include a thermal storage system.

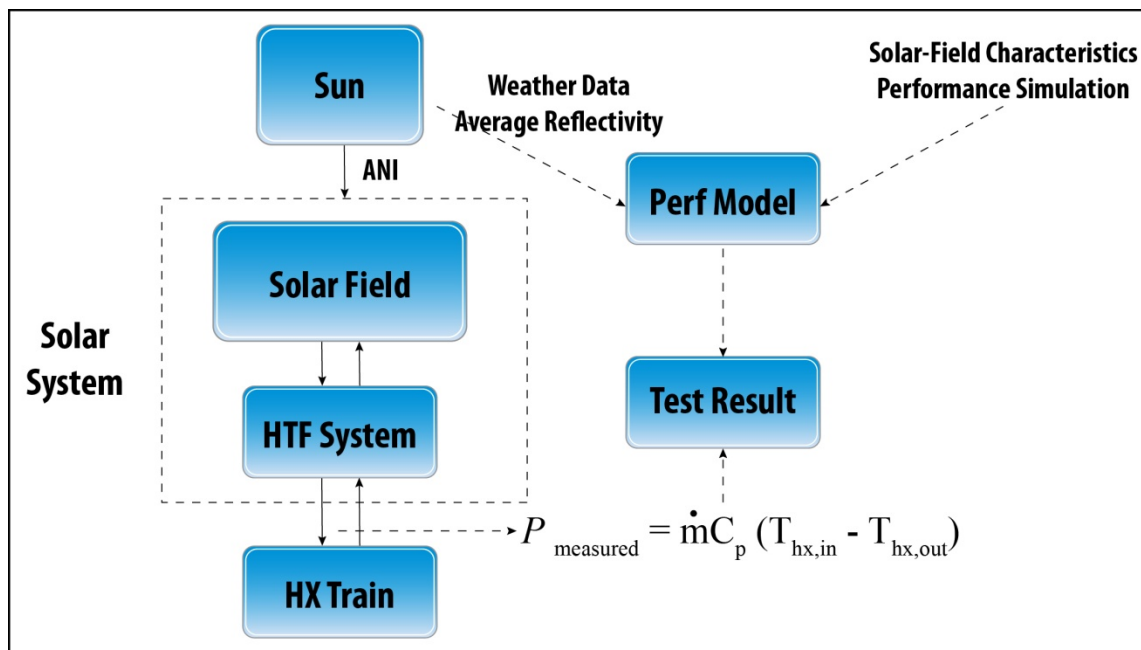


Figure ES-1. Schematic of solar system boundary and performance model

Performance acceptance tests are to be conducted with acceptable accuracy according to clearly stated procedures agreed upon between the parties involved. These Guidelines deal with issues specific to utility-scale parabolic trough solar fields. However, applicable performance test codes (PTCs) developed by ASME for other types of energy systems have very useful information for developing a detailed test plan, and are appropriately cited in these Guidelines. For example, applicable PTCs provide a general framework and information about instrumentation, data acquisition, data reduction, testing procedures, uncertainty levels, and test reports. These Guidelines focus particularly on the issues unique to the parabolic system shown in Figure ES-1.

The primary objectives of the tests are the following:

- a. Power Test—Measure solar thermal power output (including the design-point solar thermal power, or capacity, if contractually required).
- b. Efficiency Test—Measure solar thermal efficiency at the same test conditions.
- c. Compare (a) and (b) to performance model projections.
- d. Monitor bulk solar field inlet and outlet temperatures at heat-exchanger inlet(s) and outlet(s), and/or at subfield boundaries.
- e. Measure HTF system and solar system parasitic power consumption.

Two primary types of test runs are to be conducted. The first—the Short-Duration Steady-State Thermal Power Test—measures the thermal power output and thermal efficiency of the solar system under clear-sky conditions over a short period during which thermal equilibrium and stable steady-state conditions exist, and compares the measured results to performance model projections for those parameters. Important issues related to both thermal equilibrium and stabilized test conditions are dealt with in considerable detail in the Guidelines.

The second—the Multi-Day Continuous Energy Test—gathers continuous daily thermal energy output (integrated power output using Eqn. 3-1; efficiency from Eqn. 3-2) and compares the results to projections from a performance model. Both clear-sky and partly cloudy conditions are acceptable. Additionally, the functionality of the solar system should be observed with regard to such items as daily startup, normal operation, and shutdown.

Test methods are provided for both the short-term thermal power test and multi-day continuous energy test. Of special importance are the criteria that must be satisfied by the short-term power test. The recorded data can be viewed as having two components—the actual test measurements and the uncertainty interval associated with those measurements and other test conditions. Both are closely examined within these Guidelines, especially the magnitude of uncertainty in the results, and recommendations made on acceptable limits. The uncertainties in the power and efficiency results are influenced in several ways by the constantly changing energy input to the solar field, captured here in the aperture normal insolation (ANI) term.

The solar system must be in a stable thermal condition (thermal equilibrium) and stable test condition (power measurement) prior to testing. This requires stable characteristics in the:

- solar field inlet temperature
- solar field outlet temperature

- mass flow rate change stabilized with change in ANI.

These three conditions are dictated by the following influences, respectively:

- power block stability
- solar field HTF flow control system
- time duration and magnitude of the ANI gradient.

Once thermal equilibrium and test condition stability have been reached, the criteria for valid power and efficiency measurements (i.e., valid test runs) are primarily based on the level of uncertainty in the test results calculated using standard practice. Systematic uncertainties are the dominant consideration.

However, and very important, it must be recognized that the purpose of these Guidelines is to provide information so that the testing parties can settle on project-specific, agreed-upon criteria and other test issues important to the overall purpose of the tests. For any given project, the performance acceptance tests will be conducted in accordance with a Test Plan written by the testing parties. The intent of these Guidelines is to provide insights into the issues and test methods that are critical to formulating a valid Test Plan, and to lay the groundwork for accurate test results.

1 Introduction

1.1 Technology Description

Parabolic trough systems with a high-temperature heat transfer fluid (HTF) are currently the most-proven concentrating solar power (CSP) technology because of a long commercial operating history starting in 1984 with the Solar Electric Generating System (SEGS) plants in the Mojave Desert of California. Consisting of nine plants with capacities ranging from 15 to 80 MWe and a cumulative total 354 MWe, the SEGS plants continue to operate and demonstrate consistent and reliable performance. In the last several years, as a direct result of new and effective policies, project development activity in commercial parabolic trough power plants has strongly accelerated, with new plants being built in Spain and the United States. Specifically, a 1-MWe trough system was commissioned in Arizona in 2006, a 64-MWe Nevada solar plant began operating in 2007, and a number of 50-MWe facilities have begun operating in Spain. By late 2010, announced trough projects in Spain and those with signed power purchase agreements (PPAs) in the southwest United States total more than 9 GW.

Parabolic trough power plants consist of large fields of mirrored parabolic trough collectors, an HTF/steam-generation heat exchanger (HX) system, a power system such as a Rankine steam turbine/generator, and optional thermal storage and/or fossil-fired backup systems. Trough solar fields can also be deployed with fossil-fueled power plants to augment the steam cycle, improving performance by lowering the heat rate of the plant and either increasing power output or displacing fossil fuel-derived electricity. See Figures 1-1 and 1-2.



The solar field (SF) comprises large modular arrays of single-axis-tracking parabolic trough solar collectors that are arranged in parallel rows, usually aligned on a north-south horizontal axis. Each solar collector has a linear parabolic-shaped reflector that focuses the direct beam solar radiation on a linear receiver (absorber tube) located at the focal line of the parabola. For a typical north-south orientation of the collector axes, the collectors track the sun from east to west during the day, with the incident radiation continuously focused onto the linear receiver where a heat transfer fluid is heated to nearly 400°C (750°F).

Figure 1-1. SEGS IV, Kramer Junction, California.
(Photo from Luz International Ltd., circa 1990)

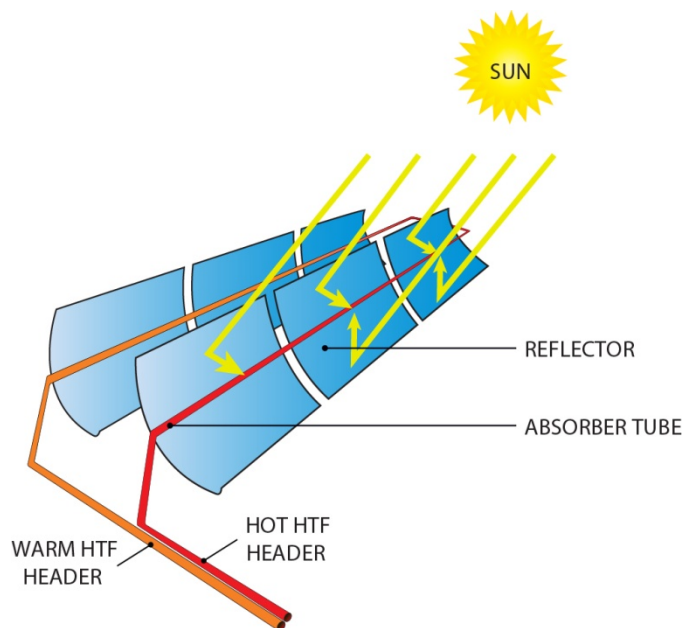


Figure 1-2. Trough collector schematic. (Illustration from Flagsol GmbH)

Because a concentrating collector must focus the sun’s rays on the receiver, the solar resource relevant to performance is the beam radiation from the sun, measured as the direct normal insolation² (DNI) on a plane perpendicular to the rays. The DNI on the Earth’s surface is reduced from the extraterrestrial level by scattering in the atmosphere caused by moisture and other particles. In a linear-axis tracking trough collector, the effective beam radiation is the component perpendicular to the plane of the aperture of the parabolic-shaped mirrors. Later in this report, we shall refer to that component as the aperture normal insolation, or ANI.³ For purposes of Acceptance Testing, it will be shown that the ANI is an important characteristic of the solar resource for the purposes of these Guidelines.

After circulation through the receivers, the HTF flows through a heat exchanger to generate high-pressure superheated steam (typically 100 bar/371°C [1450 psia/700°F]), and/or to a thermal storage system, if present. In a Rankine-cycle plant, the superheated steam is fed to a conventional reheat steam turbine/generator to produce electricity. The spent steam from the turbine is condensed and returned to the heat exchangers via condensate and feed-water pumps to be transformed back into steam. Steam condensation occurs via a surface condenser combined with an evaporative cooling tower (wet cooling), or directly in an air-cooled condenser (ACC) (dry cooling). The selection of condensation method will influence water usage, cycle performance, and capital cost. Dry cooling significantly reduces water use, but it increases investment and levelized electricity costs.⁴ After passing through the HTF side of the solar heat

² Radiation on the plane normal to the ray from the sun, where “insolation” is a term originating from “**in(coming) sol(ar radi)ation.**”

³ Use of this term is credited to remarks by Patrick Griffin of Thermoflow, Inc., Sudbury, Massachusetts.

⁴ Due to both higher capital costs of the cooling system and degraded performance during hot ambient conditions. Further, electricity revenues are lowered because the output reduction typically occurs during high-value time-of-delivery periods.

exchangers, the HTF is then reheated as it recirculates through the solar field. Current research and development (R&D) programs are exploring the use of molten nitrate salts or pressurized gases for the HTF, as well as direct steam generation in the solar field.

A unique and very important characteristic of trough and power tower CSP plants is their ability to dispatch power beyond the daytime sun hours by incorporating highly efficient thermal energy storage (TES). During summer months, for example, plants typically operate for up to 10 hours a day at full-rated electric output without thermal storage. However, as illustrated in Figure 1-3, significant additional full-load generation hours can be efficiently added or shifted if thermal storage is available, allowing a plant to meet the morning and evening winter peaks that many utilities in the southwest United States experience.

Another approach is to configure the systems as hybrid solar/fossil plants, that is, a secondary backup fossil-fired capability can be used to supplement the solar output during periods of low solar irradiance. This alternative fossil-based method to match the utility system load profile is possible because of the thermal-cycle power plants.

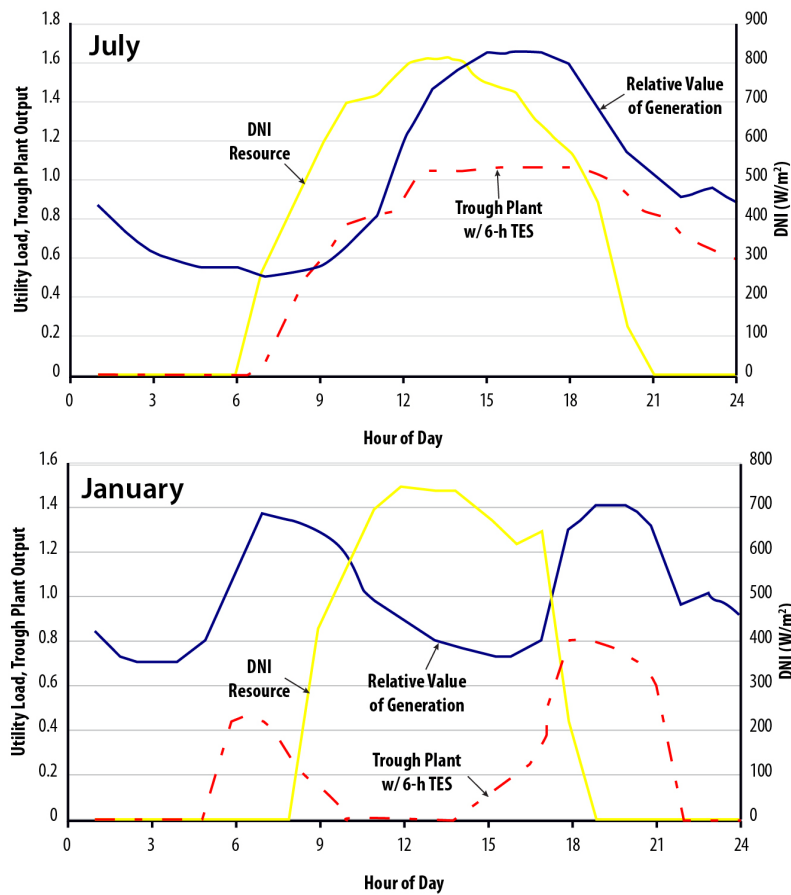


Figure 1-3. Plant operation based on utility load profile showing how TES can be used to better match the CSP plant's output to utility needs. (Graphs from Abengoa Solar)

Considerable R&D is under way and planned in all aspects of trough systems: collector component improvements, power plant integration and configuration, thermal energy storage systems, cost reduction measures, and performance improvements. Funded both by internal

company resources and by government programs, a number of innovative approaches to trough technology improvement are being developed in all these areas.

In solar trough plants that are configured with thermal storage systems, the solar field is typically increased in size to raise the energy collected. For example, on a clear day, a large solar field could provide enough energy in the morning and afternoon hours to both drive the turbine at full load all day and also charge storage to full capacity. For a given plant and utility application, the size of the solar field can be optimized for the local solar resource, grid demand pattern, electricity revenues (e.g., if time-of-use revenue multipliers are applicable), and financial parameters. For this purpose, a reference solar field size is determined at a nominal hourly DNI and solar field design parameters at rated solar thermal power capacity, and this is labeled as solar multiple (SM) = 1. Larger solar fields are identified as SM >1. For plants with no thermal storage in a high DNI region, the optimum solar field size will typically fall in the SM = 1.4 to 1.5 range. For plants with thermal storage, SM values of 2.0 and higher will typically be chosen.

1.2 Need for Guidelines

Solar thermal trough power plants are being proposed with turbine capacities as large as 280 MWe gross and, if significant thermal storage is included in the system, can require solar fields with up to 2.6 million m² of reflector aperture in an area of high solar resource, and even larger solar fields in areas of less solar resource. The land requirement for a large plant with thermal storage is about 7.5 acres (~3 hectares) per MWe net. Heretofore, developers, debt providers, owners, and engineering, procurement, and construction (EPC) contractors have had no standardized test guidance for reference or use that is specifically associated with the performance acceptance of these large and capital intensive solar fields. This need will intensify as deployment of parabolic trough systems increases in the United States and internationally.

The fundamental differences between acceptance of a CSP solar system and a conventional fossil-fired system are the transient nature of the energy source, and the need to use a performance projection model⁵ in the acceptance process. These factors bring into play the impacts of transient processes, uncertainties introduced by a model, and the need to test, or model, seasonal or annual performance within the scope of the acceptance test procedure in order to capture significant impacts on performance.

The Performance Test Guidelines presented in this report are intended to provide guidance for the planning, preparation, execution, and reporting of performance test results on large-scale (utility-scale) parabolic trough solar systems that are made up of the solar field and HTF subsystems.

It is anticipated that an official Performance Test Code (PTC) developed by the American Society of Mechanical Engineers (ASME) will, at some future time, supersede the parabolic trough Guidelines reported here. That code—ASME *PTC 52 - Concentrating Solar Power Plants*—is being planned to address other CSP technologies in addition to parabolic troughs. Typically, it takes several years to complete the preparation and approval of a PTC.

⁵ Use of a performance model in place of correction curves is also a trend in the testing of fossil-fuel power systems.

2 Objectives and Scope

The objective of this document is to provide performance acceptance Guidelines for the solar system of parabolic trough power plants. The solar system includes both the solar field and HTF system. The power block and balance-of-plant (BOP) are not within the boundaries of this protocol. *ASME PTC 46 - Overall Plant Performance* would be the appropriate code for performance and acceptance testing of the power island.

Specifics on the type, duration, and frequency of tests for a particular project should be separately defined in a test plan that is part of the contractual agreement between the party turning over the solar system and the party taking control of the solar system. The test plan is a commercial agreement that will dictate the required testing for the transaction. This Guideline has been prepared to recommend and provide guidance for several tests that can be used to meet the objectives of the contractual agreements.

2.1 Parties to the Acceptance Tests

There are a large number of commercial scenarios under which acceptance tests on the solar system would be conducted. One such possible scenario is given below for purposes of illustration and clarity. Although this example is intended to help place various steps or responsibilities in perspective, it does not imply that other, equally valid, representative scenarios do not exist. The most important point is that the objective of these Guidelines is to present viable test methods that are applicable to acceptance testing of large parabolic trough solar systems regardless of the relationships of the parties involved.

2.2 Example Project Scenario

- Test requirements are agreed upon between the EPC contractor and the solar system Technology Provider (TP). The TP is selected by the EPC contractor, either independently or by agreement with the Developer/Owner.
- The EPC contractor sequentially carries out the solar system commissioning, startup, and acceptance testing with the Owner's Engineer observance. Performance Acceptance Tests are to be conducted after the solar system is fully commissioned and operational, and is ready for turnover from the TP to the EPC.
- At successful completion, the TP then turns over the solar system to the EPC contractor.

2.3 Pass / Fail Criteria

To be clear, the criteria for passing or failing the performance acceptance tests recommended in this report are a contractual matter to be agreed upon by the parties involved.

2.4 Readiness for Acceptance Tests

While the conditions to start acceptance testing are subject to contract conditions, in a typical IPP project development the acceptance performance test of the solar system occurs after commissioning of the system by the EPC construction and startup teams. Commissioning involves mechanical, electrical, instrumentation, and functional checks and walk-throughs to bring the solar system to an operating condition suitable for commercial operation and acceptance testing. All critical punch-list items from the walk-throughs are complete at this time,

as well as most lower-tier punch-list items. When the system is fully operational and performs all required functions, it is turned over to the responsible party (e.g., the EPC startup team) for Acceptance Testing. At this point, the performance of the solar system has not yet been rigorously tested, nor the system accepted by the Owner.

2.5 Unique Characteristics of Solar System Performance Tests and the Role of a Performance Model

A performance test of fossil-fired equipment, such as a boiler or combined-cycle plant, is a steady-state test based on thermal equilibrium, characterized by a controlled, steady heat input and a measurable output. Although in practice it requires care to achieve and maintain steady-state conditions, it is greatly facilitated by the fact that the input energy is controllable. In simple terms, a steady-state test is passed if the measured capacity or efficiency of the system meets the specified value. An important characteristic of the fossil-fired power system is that it often operates at or near its nameplate capacity.

A solar system, on the other hand, is characterized by the continuous movement of the sun and the changing heat input to the solar field. This complicates the achievement of steady operating conditions during the test period. Furthermore, there are many daylight hours during the year when the solar system is not operating at capacity due to the diurnal and seasonal nature of the solar resource.

The predicted performance of the solar system depends on the exact location of the sun and the specified characteristics of the solar collectors and HTF system. Because of the variable nature of the solar resource, a performance model (computer code) is required to predict the performance for given input conditions.

A parabolic trough on a north-south axis tracks the beam radiation from the sun from morning to evening from east to west. For many promising solar plant locations the sun is never directly overhead. Because of its seasonal and diurnal position in the sky, in the winter, for example, the sun is low in the southern sky. The DNI, or direct normal insolation, is the direct beam radiation measured normal to the rays from the sun, and is independent of the collector position. The ANI, on the other hand, is the beam radiation component normal to the aperture plane of the collector. It is the energy that is useable by the collectors in the solar field, and is computed from the DNI and incidence angle, shown in the schematic diagram below. If the incidence angle is zero, the direct radiation from the sun is normal to the collector, and the ANI = DNI. If Θ is not zero,

$$\text{ANI} = \text{DNI} * \cos(\Theta)$$

A factor in the performance model called the incident angle modifier, or IAM, accounts for changes in optical properties resulting from non-normal incidence on receivers and mirrors excluding the $\cos(\Theta)$ effect above. A plot of a typical IAM curve is also shown in Figure 2-1.

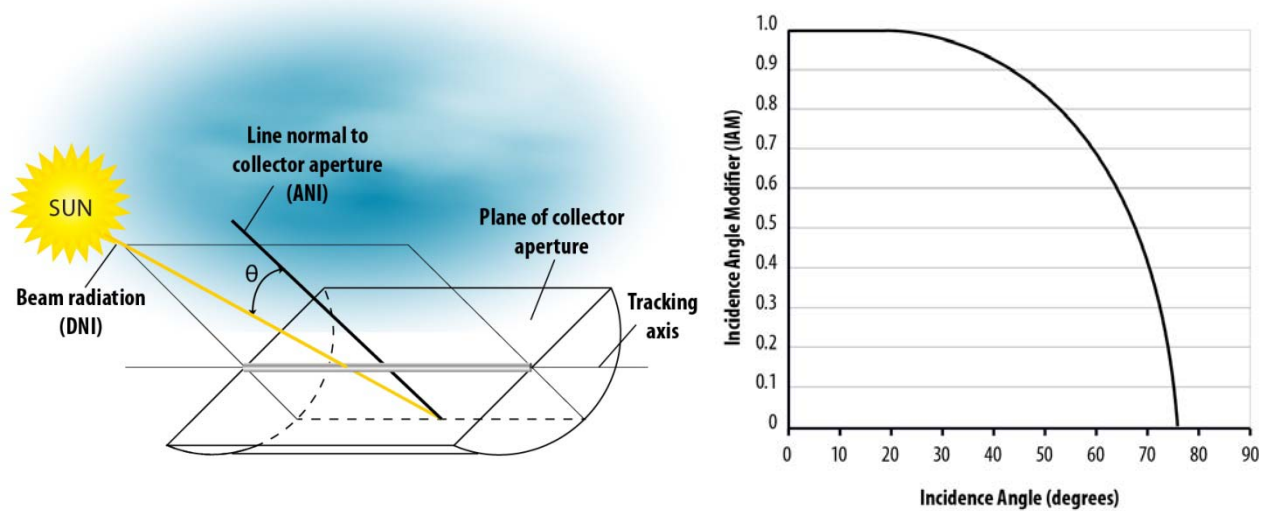


Figure 2-1. Trough energy input.

2.6 Utility-Scale Solar System Performance Acceptance Tests

This Guideline recommends a set of tests for use in the acceptance of a utility-scale solar system using parabolic trough technology. All or selected tests from this group can be chosen by agreement between the test parties. The data collected for each test are identical in nature. The tests, described in detail in Section 4, are the following:

1. Short-Duration Steady-State Thermal Power Test
2. Multi-Day Continuous Energy Test

2.7 Solar System Boundaries

The current version of these Guidelines does not include a thermal storage system. The solar system boundary is defined in this case to be the shutoff valves in the HTF piping at the inlet and outlet of the solar heat exchanger(s), as shown in Figure 2-2. The solar system comprises the solar field and HTF subsystems. The boundary between these subsystems is defined as the shutoff valves on the interconnection piping for each loop to the cold HTF header and hot HTF header, respectively, in each segment of the solar field.

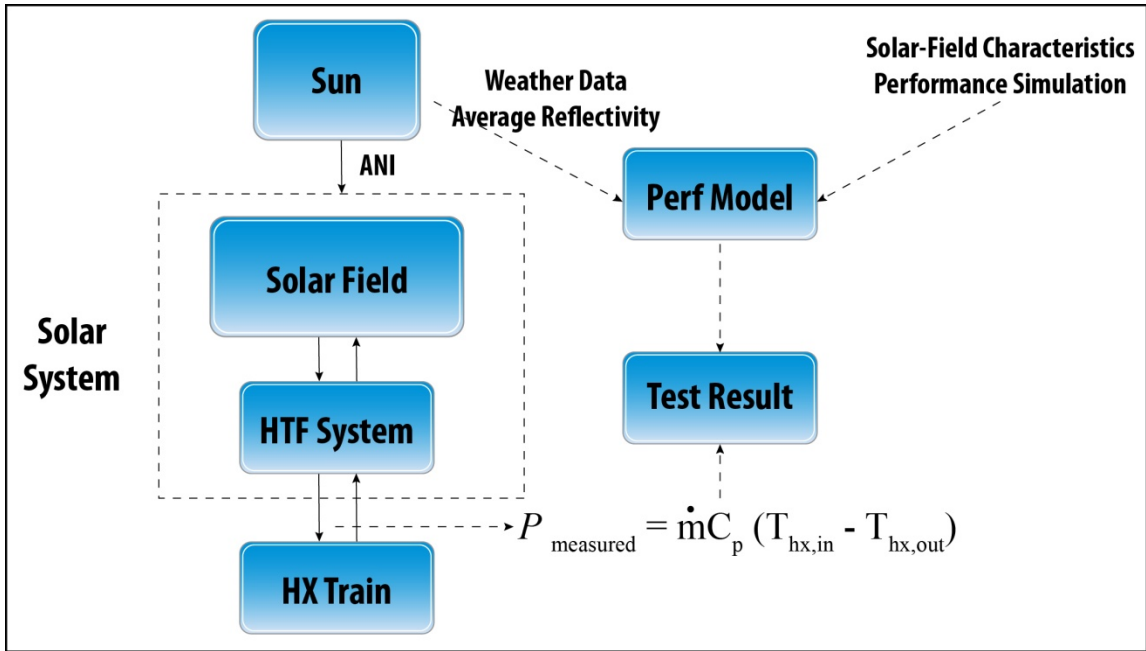


Figure 2-2. Schematic of solar system boundary and performance model.

3 Test Definitions

3.1 Performance Acceptance Test Guidelines

This section elaborates on the objectives and elements of the two types of acceptance tests for large parabolic trough solar systems identified in Section 2. Performance acceptance tests are to be conducted with acceptable accuracy according to clearly stated procedures agreed upon between the parties involved. These Guidelines deal with issues specific to utility-scale parabolic trough solar fields, for which no ASME performance test code yet exists. However, applicable PTCs developed by ASME for other types of energy systems have very useful information for developing a detailed test plan, and are appropriately cited in following sections. For example, PTCs provide a general framework and information about instrumentation, data acquisition, data reduction, testing procedures, uncertainty levels, and test reports. However, note that many details are specific to a project and need to be stipulated in the context of the overall test plan.

3.2 Short-Duration Steady-State Thermal Power Test

3.2.1 Introduction and Purpose

The purpose of this test is to measure the thermal power output and thermal efficiency of the solar system under clear-sky conditions over a short period during which thermal steady-state conditions exist, and to compare the measured results to performance model projections for those parameters. These tests are defined to be the Power Test and the Efficiency Test. (See the subsequent section, Specific Test Objectives.)

The thermal power output of the solar field during a short test period will vary primarily with the magnitude of the solar resource and the time of day and season. Secondary impacts on power output result from variations in wind speed and ambient dry-bulb temperature. It is shown later that thermal steady-state conditions can be expected at most times of the year for short test-run durations.

The purpose of this Guideline is to define or recommend methods to carry out valid acceptance tests. Criteria to judge successful completion of the tests are left to commercial agreements between the test parties.

Commercial agreements may require that, at some stage, the rated solar thermal design power (or capacity) be measured at appropriate solar resource conditions. If such conditions do not exist in the period at the end of commissioning and turnover of the solar system, then provisional acceptance tests can be carried out, with a final acceptance test to follow for rated solar thermal design power when solar conditions allow.

3.2.2 Solar Resource and Weather

The tests are to be run on clear days during any time of year. Even with a high DNI, which can be experienced on a clear winter day, the important solar resource term that dictates the thermal energy input into the solar field is the direct insolation vector normal to the aperture plane of the parabolic trough, earlier defined as the ANI. During fall through winter seasons, for example, the sun is lower in the southern sky much of the day, resulting in a low ANI even when the DNI is high. Good resource conditions suitable for rated design-point power tests will be those with an ANI near the design point. The analysis presented just below suggests that a relatively constant,

or slowly changing, ANI is experienced by a parabolic trough collector on clear days during mid-day hours at any time of year, albeit over a broad range of power levels.

During the performance test period, the solar field and HTF systems should not be operated beyond of their specified or suggested operating limits for solar resource (in terms of ANI), ambient temperature, or wind speed as provided by the solar system supplier(s).

3.2.3 Specific Test Objectives

The primary objectives of the tests are the following:

- a) Power Test—Measure solar thermal power output (including the design-point solar thermal power, or capacity, if contractually required).
- b) Efficiency Test—Measure solar thermal efficiency at the same test conditions.
- c) Compare (a) and (b) to performance model projections.
- d) Monitor bulk solar field inlet and outlet temperatures at heat-exchanger inlet(s) and outlet(s), and/or at subfield boundaries.
- e) Measure HTF system and solar system parasitic power consumption.

3.2.4 Calculations

3.2.4.1 Delivered Power Calculation

The thermal power output of the solar system is to be calculated at the solar heat exchangers, which, for a large solar plant, will be configured in a series of parallel heat-exchanger trains. For each train, the delivered thermal power can be computed from:

$$\begin{aligned}
 P_{measured} &= \dot{m} \Delta h_{hx} \\
 &= \dot{m} \int_{T_{hx,out}}^{T_{hx,in}} C_p \cdot dT \\
 &= \dot{m} \bar{C}_p (T_{hx,in} - T_{hx,out}) \quad \text{(Eqn. 3-1)}
 \end{aligned}$$

where

- P = Solar thermal power
- \dot{m} = HTF mass flow rate
- Δh_{hx} = Enthalpy difference between inlet and outlet of heat exchanger
- \bar{C}_p = Integral average specific heat of HTF
- T_{hxin} = HTF average bulk inlet temperature to solar heat-exchanger train
- T_{hxout} = HTF average bulk outlet temperature from solar heat-exchanger train

For a large solar power plant, the solar field design will likely be configured in solar system subfields that, together, make up the full solar field. In some cases, the HTF from an individual set of subfields will be collected to go to an associated set of solar steam-generator trains. The delivered thermal power measured across a set of subfields and accounting for the appropriate calculated inlet and outlet piping heat loss can be used as a check against the delivered thermal

power at the heat-exchanger train, but not as the primary measurement, unless agreed upon between testing parties.

3.2.4.2 Efficiency Calculation

The solar thermal efficiency can be based on either DNI or ANI in the denominator, as mutually agreed upon by the test parties. ANI is recommended because it is the true energy input to the field.

The solar thermal efficiency based on ANI is computed from:

$$\eta_{measured} = \frac{P_{measured}}{ANI \cdot A_{aperture}} \quad (\text{Eqn. 3-2})$$

where

- η = thermal efficiency
- θ = average solar incidence angle during a test run
- ANI = $DNI \cdot \cos\theta$
- $A_{aperture}$ = solar field aperture area in tracking mode during the test

The active tracking aperture area will be used for the $A_{aperture}$ term. Note that if the solar field condition for the test includes stowed solar collector assemblies (SCAs) then the receiver thermal losses will be abnormally high (because they are associated with the total solar field aperture area) and the efficiency result will be too low. The performance model projection should account for this condition.

3.2.4.3 HTF Solar Field Inlet and Outlet Temperatures

For completeness, measurements should include the average bulk inlet and outlet HTF temperatures at one or both of the following:

- Each heat-exchanger train (primary measurement)
- Each solar field subfield (secondary measurement).

The heat-exchanger test is noted as “primary” because it gives the solar field power at the point of delivery to the power block. Measurement at the subfield level (“secondary”) requires a correction for heat loss in the headers to arrive at an equivalent value.

3.2.4.4 HTF Physical Properties

Calculation of the mass flow typically requires measurement of the volumetric flow rate and knowledge of the HTF density as a function of temperature. Calculation of the thermal power also requires knowledge of the HTF specific heat. These fluid properties of the HTF, although available from the manufacturer for fluid that meets as-new specifications, should be measured prior to the test per agreements between the test parties. These measurements are even more

important for performance tests that are run on solar systems where possible HTF degradation may have occurred (e.g., from off-design operation of the ullage⁶ system).

3.3 Multi-Day Continuous Energy Test

The objective of this test is to gather continuous daily thermal energy output (integrated power output using Eqn. 3-1; efficiency from Eqn. 3-2) and to compare the results to projections from a performance model. Both clear sky and partly cloudy conditions are acceptable. Conditions in which cloud cover unevenly affects portions of a large solar field will need to be treated on a case-by-case basis, and agreed upon by both parties. In the event of multi-day fully cloudy or rainy weather—and perhaps in the event of non-uniform shadowing, as mentioned above—the test should be terminated and then restarted when appropriate. Additionally, the functionality of the solar system should be observed with regard to such items as daily startup, normal operation, and shutdown.

It is recommended, based on similar typical tests on power systems, that the test be a continuous 10-day test with data acquisition on 10-second intervals (i.e., test readings) to accurately capture morning startup, evening shutdown, and weather events. However, there is no hard, strong justification for these time durations or intervals, and specifics on duration of the test, data acquisition requirements, and contingencies in case of operational problems are to be agreed upon between the testing parties. It is also recommended that a stop/start pattern be permitted if other circumstances not related to the solar system require that the test be temporarily suspended due to, for example, shutdown of the power block.

The measured energy output results over time are to be compared to the same values as predicted by the performance model agreed upon by both parties, e.g., the model that was used for pro-forma calculations and delivered by the equipment supplier or EPC contractor at contract signing. The input values to the performance model are also to be agreed upon by both parties and are to include the local DNI data and other appropriate weather conditions, specified warranty characteristics of the solar field, and mutually acceptable adjustments for the operating condition of the solar field (e.g., number of collectors not available). Treatment of the reflectivity values of the reflectors is discussed in Section 4.2.2.

Because of the use of a performance model, no test-correction curves are involved because the model contains internal algorithms that adjust for off-design conditions. The contract shall define any commercial tolerance (which may or may not be linked to test uncertainty) allowed for in the pass/fail criteria (to be specified in the Test Plan).

3.4 Performance Model Projection and Comparison to Measured Results

The performance model used for the acceptance test must be mutually acceptable to both test parties, and typically would be the identical model using the system characteristics also used for the project financial projections. The input parameters for the performance model should be

⁶ The HTF expansion vessel(s) have an ullage volume above the liquid HTF pressurized to 10 bar to prevent boiling at 393°C. This volume contains primarily HTF vapor and nitrogen, along with limited degradation products due to a very slow thermal decomposition of the HTF, resulting primarily in free hydrogen and a few other light hydrocarbons. The ullage system is designed to maintain the ullage volume pressure in the expansion vessel(s) and process the degradation products.

identical to those used in the commercial projections for the power plant. The weather file—DNI, wind speed, ambient dry-bulb temperature—should be the actual weather file with the time stamps perfectly synchronized with the measured test data.

The possible exception to this rule is the soiling condition of the solar field reflectors. This issue is treated in Section 4.2.2.

The comparison of the measured capacity or efficiency to the model-projected value must take into account the uncertainty intervals for each quantity.⁷ The measured quantity has an uncertainty interval associated with it, and the result is a band defined by the measurement plus or minus (\pm) its uncertainty interval.

The same is true of the value projected by the performance model. Because the performance model is the same as that used in the commercial projections, it is taken to have no uncertainty except that associated with the weather input and average mirror reflectivity value. Validation of the model algorithms and accuracy is a matter between the testing parties and is outside the scope of this Guideline. Although ambient temperature and wind speed could be taken into account, it is the parameters in Eqn. 3-1 that dominate the uncertainty.

The uncertainty band for the result is very important and must be given in the test results. Comparison of the measured value to warranted levels—and whether or not the test uncertainties are incorporated into this comparison—is a commercial issue to be agreed to by the parties and is beyond the scope of these Guidelines or ASME PTCs.

3.5 HTF and Solar System Parasitic Power Consumption

This measurement is for information, unless otherwise guaranteed, and should include the instantaneous total parasitic power requirement of the HTF system, as a function of flow rate, during each test period and test run (a subset of the test period). Similarly, the solar field parasitic for the drive system should be measured.

⁷ That is, the uncertainty bands need to overlap for a valid test run.

4 Test Methods

4.1 Introduction

Ideally, the performance tests should be in thermal equilibrium and at a steady state condition. Neither goal is completely possible due to the effects of a changing heat source and changing ambient conditions. Failure to achieve either goal contributes to uncertainty in the test results.

ASME Performance Test Codes 4 and 46 assert that thermal steady-state is defined as an operating condition in which the system is at thermal equilibrium, and that the guiding criterion for steady-state test conditions is that the average of the data reflects equilibrium between energy input and energy output to thermal and/or electrical generation. The continuously varying energy input from the sun, combined with other solar field characteristics, make this a particularly challenging objective.

The receivers and entire subfield react fairly quickly to a change in the solar field heat input, or ANI. The main issues affecting thermal equilibrium are the heat exchange between the HTF and the headers (both walls and insulation) in the long header runs from the subfields to the power block, and warming or cooling of the HTF itself. Controlling a constant HTF outlet temperature at the exit of the subfields will greatly facilitate achieving thermal equilibrium in the headers. Because of the near-incompressibility of the HTF, the mass flow rate changes very rapidly throughout the entire solar field when the pump speed is changed, facilitating the HTF subfield exit temperature control. The objective in this regard is that the measurement of the ANI power to the solar field corresponds with the measurement of power delivered to the heat exchangers at the same point in time. With a changing ANI, errors will be introduced that add to the uncertainty of the result, as discussed in Section 4.4.3. However, a stabilized (steady-state) condition for purposes of performance testing is somewhat more difficult to achieve. Several key factors contribute to this issue:

- Variations in the ANI input to the solar field
- Solar field inlet temperature variation
- Solar field outlet temperature variation
- Thermal inertia within the subfield itself, that is, the response time of the subfield outlet temperature to a change in ANI.

A crucial premise of this Guideline is that during short test runs, the combined effects of small variations in these conditions, along with the HTF outlet temperature flow control, can satisfy the requirements needed to reach a steady-state condition adequate for testing. The following paragraphs treat these issues more specifically.

4.2 Solar Field Test Conditions

4.2.1 Solar Field Area, Thermal Power Output, and Design Capacity

Typically, the solar field will be larger than required for delivery of rated design solar thermal power during late spring and summer.⁸ At the high ANI levels, the peak solar thermal power output of a solar system with a high solar multiple will often be at or above the design capacity for a properly performing solar field. In practice, however, the allowable thermal output is nominally constrained by the design thermal input of the power block and the associated turbine-cycle heat rejection at its design conditions. To control this condition, the solar field thermal output can be reduced by defocusing⁹ individual SCAs to limit the thermal output to that which the turbine can accommodate at full load. The test plan should specify the exact procedure to be used under such high insolation conditions.

If the test parties agree that demonstration of the full design capacity of the solar system is a requirement, the Thermal Power Test should be run at the rated design solar thermal output specification if possible, with the measured results compared to the projection of the solar performance model using the tracking aperture area of the solar field.

For lower-insolation periods during the year, the solar thermal output may be less than the rated design output, though useful for efficiency demonstration purposes. If required by the test parties, final acceptance of the solar system may require a test at a time of year when a higher ANI condition occurs and the performance model indicates that design solar thermal output can be achieved.

4.2.2 Solar Field Reflectivity

The solar thermal output of the solar field is directly proportional to reflector soiling, which is characterized in most solar performance models by a soiling factor.¹⁰ The projected performance of the solar field at the time of contract signing is typically based on a specified average

⁸ In solar trough plants that are configured with thermal storage systems, the solar field is typically increased in size to raise the energy collected. For example, on a clear day, a large solar field can provide enough energy in the morning and afternoon hours to both drive the turbine at full load all day and also to charge storage to full capacity. For a given plant and utility application, the size of the solar field can be optimized for the local solar resource, grid demand pattern, electricity revenues (e.g., if time-of-use revenue multipliers are applicable), and financial parameters. For this purpose, a reference solar-field size is determined at a nominal hourly DNI level and at solar-field design parameters, and this is labeled as solar multiple (SM) = 1. Larger solar fields are identified as multiples of the SM. For plants with no thermal storage, the optimum solar-field size will typically fall in the SM = 1.4–1.5 range. For plants with thermal storage, SM values of 2.0 and higher will typically be chosen.

⁹ That is, placing collectors out of focus on the sun in the stow position or in a “follow-mode,” in which the collectors continue to track but are completely out of focus at a few degrees behind the sun’s movement. Placing a collector in a “feathering” or partially off-focus position to control the outlet temperature is not a suitable strategy during an acceptance test, because this does not allow a quantitative count of the SCAs in and out of focus. Therefore, for acceptance test purposes, the solar field must have SCAs fully in or out of focus and the active solar field should be maintained constant during the test.

¹⁰ The soiling factor is one of a number of factors in the optical efficiency term of the collectors.

reflectivity. The decision on the cleaning and reflectivity measuring issue is very important to both the performance of the solar field and the uncertainty in the results.

In normal operation, the reflectors are cleaned according to methods and a wash frequency that are specific to the site location, operation and maintenance (O&M) organization, and optimization of water and labor costs versus performance gains. Mirror reflectivity is typically returned to a high level after cleaning.

For acceptance testing, agreements need to be reached between the testing parties on (a) reflector washing during the test period and (b) the soiling factor used in the model for comparison to the measured power delivery. At the time of acceptance testing of the solar system, the power plant will be operational—otherwise, it would be not be possible to reject the collected energy.

One approach could be that the solar field collectors could be washed on a schedule similar to that proposed for normal operation. That is, prior to and during the multi-day test period, operators would wash the solar field mirrors using the normal planned O&M schedule and procedure in the solar field O&M plan. For a large plant, it could take one or several weeks to complete the washing cycle. A second choice could be to carry out no reflector panel washing at all during the short-term power test or multi-day test periods.

Regardless of the approach to mirror washing, sufficient reflectivity readings should be taken to characterize the average reflectivity of the solar field for use in the performance model, with an appropriate uncertainty interval applied to the average solar field value. The testing parties need to agree on methods to optimize the spatial sampling to obtain a valid statistical average. This will likely require an additional quantity of instruments beyond the normal number at the plant. It is not possible in this general Guideline to specify in advance the number of required readings because of the site-specific character of both the solar field configuration and the soiling mechanisms at the site.

And, further complicating this issue, to our knowledge no authoritative work has been carried out on methods to determine statistically valid reflectivity averages in large trough solar fields using a reduced number of readings. In the near future, NREL expects to be working with Sandia support to develop useful approaches regarding this problem. To date, a paper touching on this subject was published in 2006 for a test project on a small power tower heliostat field at the Plataforma Solar de Almeria test facility in Spain.¹¹ Also, experience was gained at the Kramer Junction SEGS plants in the 1990s, where specific SCAs to be measured were chosen at random based on a pattern regarding the area of the solar field from which they were selected. Four SCAs were chosen from the exterior zone near the edges of the field where degradation rates are higher, whereas eight SCAs were selected from the interior zone, and the final eight SCAs were selected from the intermediate zone characterized by medium degradation.¹²

¹¹ Fernandez-Reche, J., “Reflectance measurement in solar tower heliostats fields,” *Solar Energy* 80 (2006) 779–786.

¹² Cohen, G; Kearney, D.; Kolb, G. “Final Report on the O&M Improvement Program for CSP Plants”, excerpt from Appendix E on Mirror Cleanliness, Sandia National Laboratory Albuquerque, SAND99-1290, June 1999.

4.2.3 Seasonal Example of Hourly ANI Variations

The following analysis presents data on variations in ANI on a parabolic trough collector surface for clear days during several seasons of the year. The primary result is that the ANI variation appears to be within reasonable and acceptable bounds even in winter periods. In other words, a small variation in the ANI does not necessarily preclude attainment of adequate thermal steady-state conditions. However, it is clear that the design and operation of the parabolic trough solar field must include the ability to control the bulk HTF outlet temperature at a near-constant value to achieve that state.

With clear skies, there will be no cloud transients, and with HTF flow control the solar field outlet temperature will be held within close bounds. The temperature will not fluctuate much because the controlled small changes in mass flow will be near-instantaneous throughout the HTF system because the synthetic oil is, for all practical purposes, incompressible. By these means, there will be negligible heat exchange between the header pipe walls and the HTF fluid, and therefore, no thermal capacitance effects in the headers. The change in HTF mass flow rate will follow the variation in the ANI—that is, as the ANI changes, the HTF mass flow rate will be automatically adjusted accordingly after a short delay.

The change in ANI was analyzed to examine the stability of the heat input to a trough collector for short periods in different seasons. Analysts used 1-minute, accurately measured DNI data from the NREL Solar Radiation Research Laboratory in Golden, Colorado, to show example patterns in ANI for clear days during June, March, and December for the entire day (Figure 4-1(a)) and for the daytime period between 8 a.m. and 4 p.m. (Figure 4-1(b)). Also shown in Figure 4-1(c) are the percent changes in the ANI over the previous 30 minutes during the daytime period for these three months. These results show that the variations in ANI over short time periods, e.g., 15 to 30 minutes, are relatively small during certain periods, often within a few percent.

We believe these results support the basic premise that a slowly changing heat input (ANI) and no transient heat exchange in the headers between fluid and pipe will allow valid measurements of power and efficiency at any time of year, averaged over short test runs of about 30 minutes in duration. However, if a demonstration of design-solar-system thermal power capacity is required, tests for that condition will likely need to be run in higher ANI periods. Furthermore, with continuous data acquisition and reduction on small time steps (e.g., 1-minute), the performance of the solar system can be accurately tracked and observations made on the steadiness of the results.

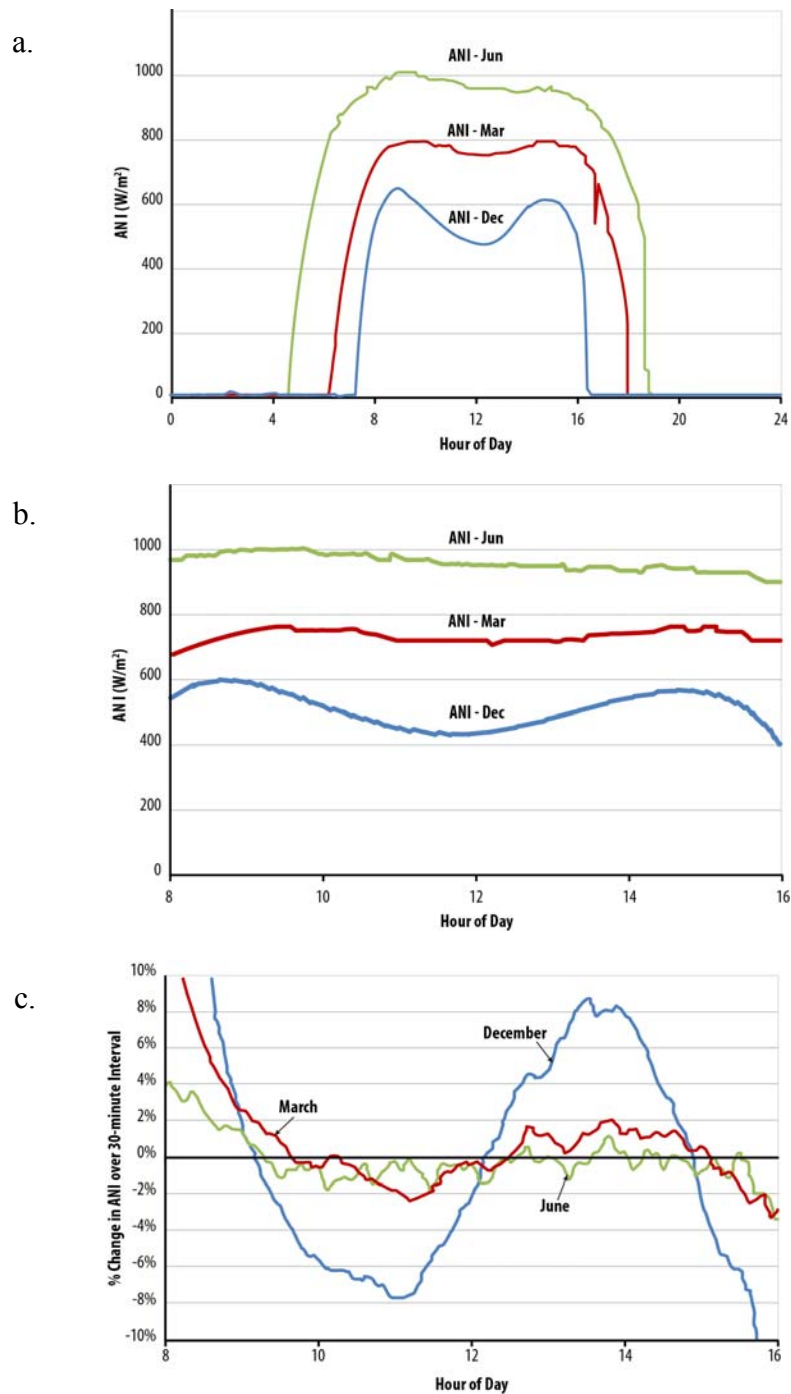


Figure 4-1. Patterns from ANI analysis: (a) during June, March, and December for the entire day, (b) for the daytime period between 8 a.m. and 4 p.m., and (c) the percent changes in the ANI over the previous 30 minutes during the daytime period for these three months. Location: Golden, Colorado. (Courtesy of NREL)

4.3 Criteria for Adequate Test Durations and Conditions

Variations in the key test parameters should be low enough to contribute only in a minor way to the uncertainty band in the results. The solar system must be in a stable thermal condition (thermal equilibrium) and stable test condition (power measurement) prior to testing. This requires stable characteristics in the:

- solar field inlet temperature
- solar field outlet temperature
- mass flow rate change stabilized with change in ANI.

These three conditions are dictated by the following influences, respectively:

- power block stability
- solar field HTF flow control system
- time duration and magnitude of the ANI gradient.

Once thermal equilibrium and test condition stability have been reached, the criteria for valid power and efficiency measurements (i.e., valid test runs) are primarily based on the level of uncertainty in the test results calculated using standard practice. Systematic uncertainties are the dominant consideration.

Table 4-1 shows an illustrative set of stabilization criteria for these conditions based on the influence of the variability of the test parameter on the total uncertainty of the test results (see Section 6, Evaluation of Measurement Uncertainty, for more details on uncertainty analysis). The variability defined in Table 4-1 is defined as the standard deviation of the mean $s_{\bar{x}}$ as described by Eqn. 6-1 divided by the average value of the parameter over the test run period. Based on the examples provided by Tables 6-1 through 6-4, a combination of the allowable variations given in Table 4-1 will result in a negligible increase in the total uncertainty of the result. It cannot be overemphasized, however, that final stabilization criteria for a specific project will be strongly influenced by the design of the solar system and associated instrumentation, and finally determined by the agreements between the testing parties.

Table 4-1. Example Stabilization Criteria for Short-Duration Steady State Power Tests of a Utility-Scale Parabolic Trough Solar Field

| Parameter | Allowable variability over test period $s_{\bar{x}}/\bar{x}$ (%) |
|---|---|
| HTF volumetric flow rate, m ³ /s | 0.5% |
| ANI, W/m ² | 0.5% |
| Solar field inlet temperature | 0.2% |
| Solar field outlet temperature | 0.2% |

These criteria are to be applied to evaluate test conditions for stability. In general, referring to Figure 4-1, the potential test period for any given day will occur between 9 a.m. and 4 p.m.

Observation of data collected from several operating plants indicates that the variability will be much smaller than the values described in Table 4-1. For example, 5-second ANI data collected over a 15-minute period (180 data points) varied by approximately $\pm 2.5 \text{ W/m}^2$ from an average value of 960 W/m^2 . The related standard deviation of the data was 1.46 W/m^2 . For this instance, the variability as defined in Table 4-1 is calculated by dividing the standard deviation of the mean ($1.46/\sqrt{180}$) by the average ANI value of 960, resulting in a variability of 0.01%.

An estimate of the time necessary to establish thermal equilibrium within a typical solar field was derived using NREL’s Solar Advisor Model. The model was run using 5-second time steps to capture the impact of transient effects resulting from a sudden change in solar field inlet temperature. Figure 4-2. describes the result of an analysis in which the error in a 15-minute average measurement of solar field power, caused by non-equilibrium conditions, is estimated based on varying step changes in inlet temperature. In the figure, $Q_{sf,abs}$ is the power (15-minute moving average) absorbed by the solar field and includes the energy absorbed by the solar field, less all thermal losses from the receivers, solar field, and header piping. $Q_{sf,del}$ is the average power delivered to the steam generator. If the solar field is not in equilibrium, e.g., the temperatures of the solar field HTF and the piping/insulation are still changing over time, the delivered power will be less than the absorbed power because some of the excess energy is used to heat the solar field HTF and piping.

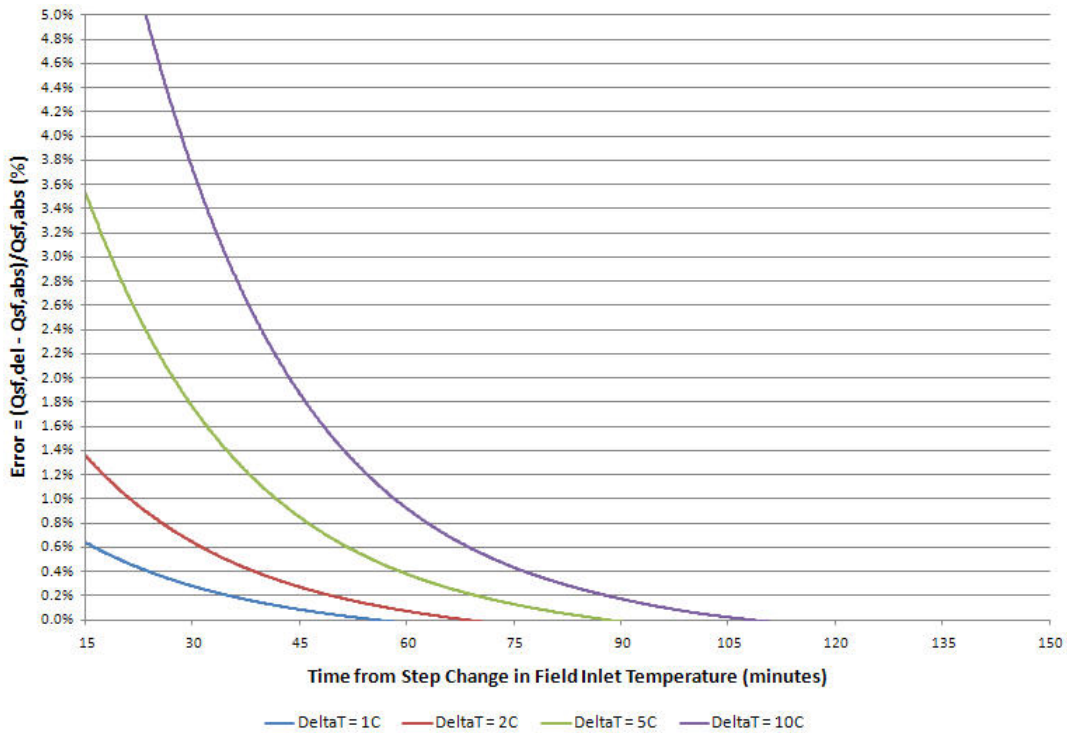


Figure 4-2. Schematic representation of HTF system elements.

Using Figure 4-2. as a guide, we can estimate the time required to minimize the error associated with non-equilibrium conditions to an acceptable level. For example, to limit the error to 0.1%

for a 1°C step change in inlet temperature, approximately 45 minutes is required to establish adequate equilibrium beyond the initial upset, depending on pipe and insulation mass. Table 4-2 gives our recommendations for a pre-test period to show stability, duration of test runs, data sampling rate, number of test points, and allowable ambient conditions within a test run period.

Table 4-2. Example Conditions for Testing Periods, Durations and Data Points for Short-Duration Steady State Power Tests

| | |
|----------------------------------|-----------------------------|
| Daily Test Period | 0900-1600 (9a.m.-4p.m.) |
| Pre-Test Steady-State Run Period | Approx. 30-45 minutes |
| Test Run Duration | Approx. 15-30 minutes |
| Test Run Data Points | 10-second averages |
| # of Test Points in Test Run | 90 - 180 |
| Maximum Wind Speed | Approx. ≤ 13 m/s |
| Minimum ANI | Approx. 500 W/m^2 |

4.4 Criteria for Valid Test Results

A valid test result must satisfy the requirements of thermal equilibrium, stabilized test conditions, suitably low uncertainty, and repeatability. Valid test run results, over approximately 15 to 30-minute durations, obtained during a single stable test run period should be averaged. Invalid test runs are those for which the run uncertainty intervals are not within acceptable limits, or if the test run result falls outside the uncertainty intervals of the test runs being compared. A limit should be set by the testing parties on the number of outlier test runs permitted.

4.4.1 Thermal Equilibrium and Stabilized Test Conditions

The criteria applied to the pre-test run period, and illustrated in Table 4-1, must continue to be satisfied through the test run period.

4.4.2 Repeatability

Repeatability of multiple test run results lends confidence to the methods incorporated in the testing. Accounting for the requirements for equilibrium and steady-state conditions, numerous 15- or 30-minute test run results can be taken within the daily 7-hour test window.

Invalid test runs are those that individually have total uncertainty intervals outside acceptable limits, or for which the test results do not lie within the uncertainty intervals of each other. A limit should be set on the number of invalid test runs that are permissible during a test run period, e.g., 10%.

It is recommended that this pattern be conducted during the best daily time periods (function of season) and repeated on three separate days during a 10-day window. In practice, once the solar system test conditions are set up, the data acquisition system can be run continuously during the full test-run period on the selected days, and the data can then be examined for suitable periods that satisfy the test run conditions for stability.

The results of each test run, or an average of test runs close together in time, should be compared to the performance model output(s). However, the uncertainty of the average calculation will be the same as the uncertainty of an individual result.

4.4.3 Impact of ANI Variation on Trough Transient Behavior

Under conditions of a continuously changing ANI, achieving true steady-state conditions during a short-duration acceptance test is not possible and therefore the impact of varying ANI on an acceptance test must be understood.

As discussed throughout this report, the solar field acceptance test seeks to compare the measured solar field thermal output to predicted output using a performance model or correction factor. The measured thermal output considers the state of the HTF at the inlet and outlet of the power cycle heat exchangers and uses a first-law energy balance to calculate the total thermal power supplied to the power cycle. This measured data is compared to the predicted solar field output, given a particular solar resource level, the solar position, and ambient conditions.

This relationship is shown in Eqn. 4-1, where the measured energy on the left as described earlier in Eqn. 3-1 is compared to the model-projected energy on the right based on the measured ANI and, in this case, thermal efficiency projected by the model. Any disparity between the left hand side (LHS) and the right had side (RHS) of the equation indicates disagreement between observed and modeled thermal power.

$$\dot{m} \bar{C}_p (T_{hx,in} - T_{hx,out}) = ANI \cdot A_{aperture} \cdot \eta_{thermal} \quad (\text{Eqn. 4-1})$$

The variables in this equation are identical in definition to those defined previously in equations 3-1 and 3-2. The percent disparity between instantaneous and observed energy can be expressed as $(\text{LHS/RHS} - 1) \times 100\%$, and results reported in the following discussion make use of this definition.

Because parabolic trough systems require extensive piping, any energy absorbed within the HTF must often travel long distances before returning to the power cycle. Because changes in ANI levels will not be observed at the outlet of the solar field piping immediately, some time lag is always present between the observed delivered energy and the instantaneous operating conditions. To understand the impact of time lag on transient performance, NREL developed a model that considers the flow of HTF through a representative solar field collector piping system, the details of which will be published separately as an NREL technical report. The NREL model tracks a large number of discrete “plugs” of HTF as they flow through the piping system at a constant velocity. Each plug of HTF interacts thermally with piping and insulation along the flow path, and incorporates a residence time at each calculation node to mimic the actual time delay observed in real piping systems.

Acceptance testing procedures may allow data collection either at the inlet/outlet of the power cycle heat exchangers or at the inlet/outlet of a single subfield, as shown in Figure 4-3. . Consequently, transient behavior at both locations is of interest. The analysis presented here is carried out for both data collection locations. The subfield boundary is selected to exclude the long-section header piping running from the power-cycle heat exchangers to the subfield header. As expected, the transient response for the smaller subfield boundary test is truncated relative to the larger solar field boundary at the heat exchangers.

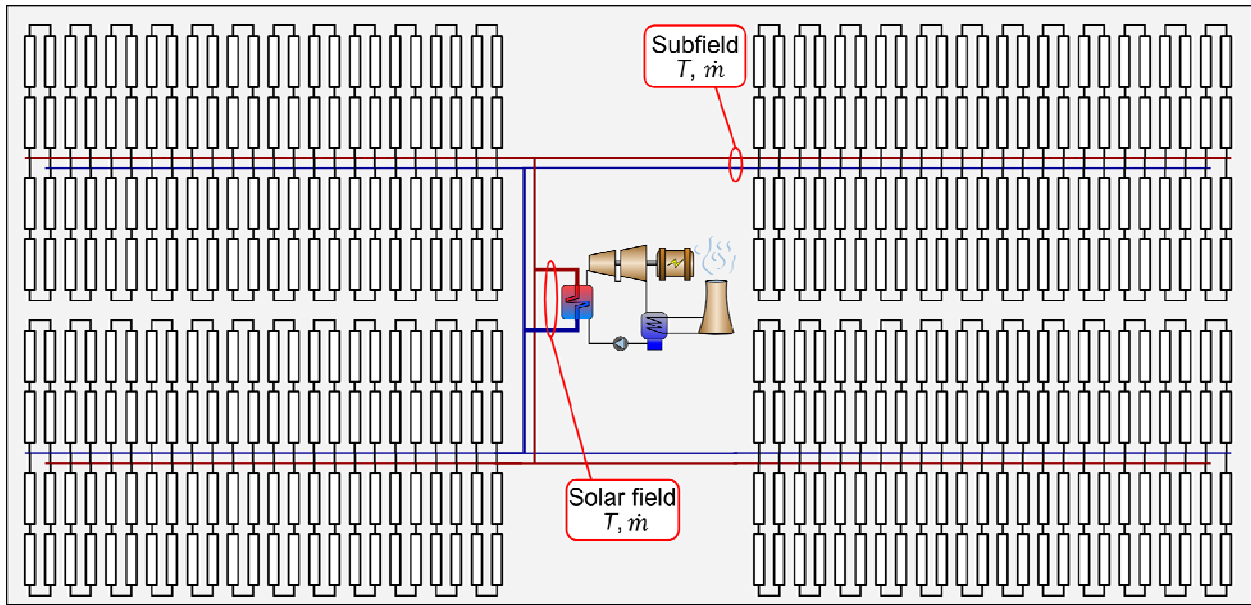


Figure 4-3. Location of two possible test boundaries for the acceptance testing procedure.

Simulation results: A number of cases—not all shown here—were analyzed to test the validity of the model against a physical understanding of solar field operation and at limits where the results could be readily compared to reality. For example, a default case was run with no ANI perturbation applied. The behavior showed that after 60 minutes the measured solar field thermal power matched the predicted solar field thermal power to within about one tenth of a percent. This behavior represents typical solar field startup conditions and is consistent with results described previously in this report. The conditions at the heat exchangers were reasonably stable after approximately 40 minutes, with slightly less than 1% disparity, while the subfield conditions were stable after approximately 25 minutes.

The results indicate, as expected, that the thermal inertia of the header piping and insulation can be a significant contributor to the amount of time that the system takes to stabilize. Next, a case was run for a system with no thermal inertia in the piping and insulation, that is, with an active mass flow control. This case is indicative of the response time for a system beginning at steady state, and maintaining a desired HTF outlet temperature throughout the simulation by varying the HTF mass flow rate as required. Under this condition, the temperature gradient throughout the loop remains constant even under varying ANI conditions; therefore, thermal exchange between the HTF and the surrounding piping is negligible. The calculated transit times compare well with the steady-state time of 8.3 minutes for the entire solar field and 5.2 minutes for the subfield.

In reality, the ANI slowly increases or decreases over the course of the acceptance test, causing a continual mismatch between the observed delivered thermal power and the modeled incident power. This condition is simulated by applying a gradient to the ANI value once the system reaches initial steady-state conditions. To estimate gradients observed during different testing scenarios, we derived representative 30-minute ANI gradients for a summer, spring, and winter day using ANI data included in Figure 4-1. Figures 4-4 and 4-5 show the results of varying the ANI rates for clear days in December and March. In these plots, ‘dt’ is the length of time

variation since the ANI perturbation was applied, and the inset is an expanded view of the period of time after 50 minutes from the start of the simulation.

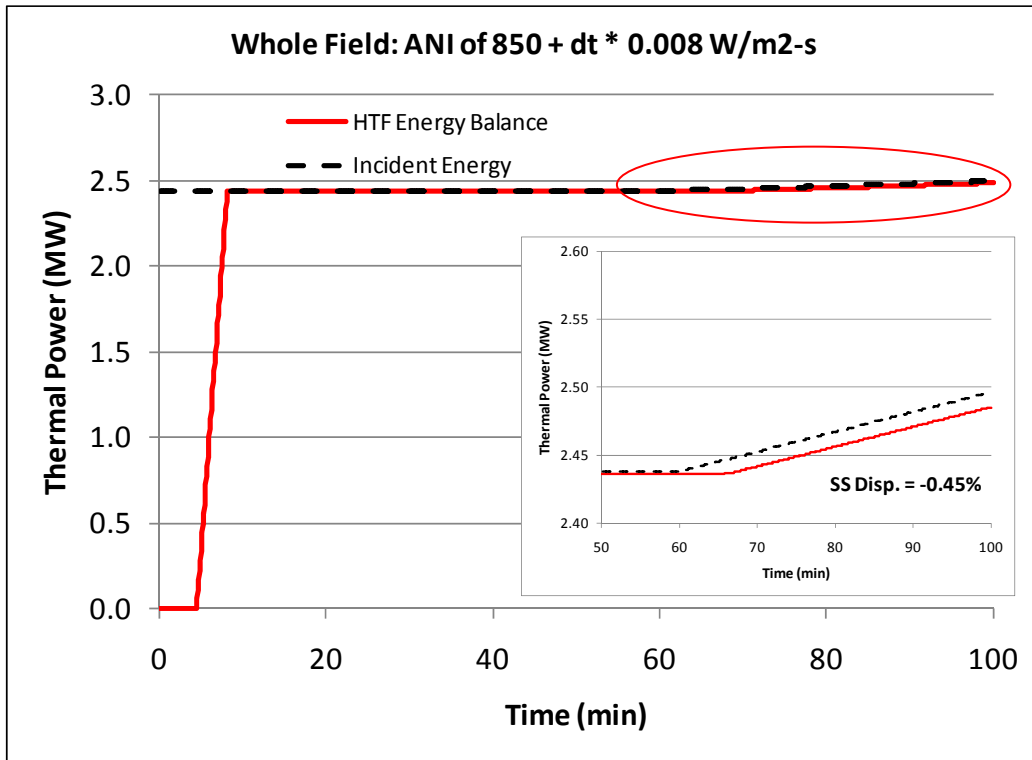


Figure 4-4. Transient response of a steadily increasing ANI (typical December) in a system with ideal mass flow rate control.

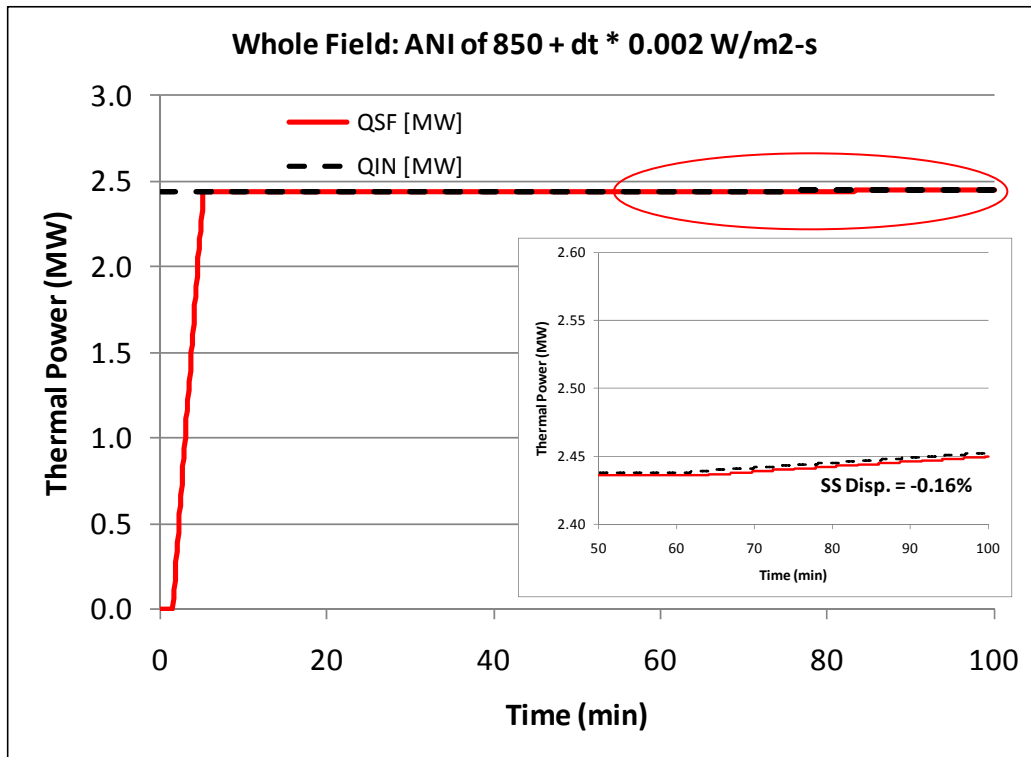


Figure 4-5. Transient response of a steadily increasing ANI (typical March) in a system with ideal mass flow rate control.

The resulting disparities for each case are presented in Table 4-3, assuming a system with ideal mass flow rate control. For comparison, the ANI gradient that corresponds to a steady-state disparity of 1% is also included. Note that these results are dependent on the base ANI level—850 W/m² in this case—and the geometry of the solar field. An increase in the incident thermal energy will cause a corresponding decrease in the steady-state disparity.

Table 4-3. Summary of Results for Several Representative ANI Gradients

| Case Description | Whole field | | Subfield | |
|---------------------------|------------------------------|---------|------------------------------|---------|
| | Gradient W/m ² -s | Disp. % | Gradient W/m ² -s | Disp. % |
| March resource profile | 0.00214 | 0.16 | 0.00214 | 0.12 |
| June resource profile | 0.00743 | 0.40 | 0.00743 | 0.24 |
| December resource profile | 0.00848 | 0.45 | 0.00848 | 0.27 |
| 1% limiting case | 0.02080 | 1.00 | 0.03900 | 1.00 |

Note that all the errors from the equilibrium effects shown here fall below 0.5%.

One potential pitfall in conducting acceptance testing during off-peak seasons is that the solar resource is typically significantly lower than during the summer months. While the DNI resource is still high in winter, the cosine (Θ) effect reduces the ANI resource considerably. During the January period, the ANI is approximately half of the 850 W/m² assumed throughout the analysis

presented above. A reduced thermal resource results in a reduced field flow rate, and all transient effects are correspondingly drawn out.

5 Instrument Selection

5.1 Required Data

The defining equations for the solar system acceptance tests are straightforward. The power output of the solar system is calculated from Eqn. 3-1 for both types of tests. Eqn. 3-2 adds the need for measurement of the DNI, and the model input data require measurement of the reflectivity of the mirrors. Together, the tests require the measurement of or accurate data on the following:

- HTF volumetric flow rate
- HTF physical properties of density and specific heat (as agreed upon by the test parties)
- HTF temperature
- Direct normal radiation (ANI is calculated from this value and $\cos(\theta)$)
- Mirror reflectivity
- Ambient wind velocity (and optionally direction), dry-bulb temperature, and relative humidity
- Latitude and longitude of the DNI instrument
- Solar system parasitic power (including both HTF system and solar field)
- Year, day of year, time of day.

Following ASME PTC guidelines, these values are defined as primary or secondary variables in Table 5-1, and the source of the data is indicated. Primary variables are those that are required to calculate the results of the test. Secondary variables are variables of interest but are not required to calculate results.

5.2 Reference Solar Field Configuration and Measurement Conditions

The piping sizes and temperature levels in a utility-scale solar system can limit the type of flow- and temperature-measurement devices that are suitable for use in that environment. A large solar field is typically divided into subfields, or sections, to optimize the field layout and header design. Large pipes are required to carry the HTF to and from the subfields from the heat-exchanger area. Operating temperatures are on the order of 300°C at the inlet to the solar field, and 400°C at the outlet from the solar field (570°F and 750°F, respectively). Header sizes could vary from 61 to 91cm (24 to 36 inches) depending on design. The size of the headers feeding the heat-exchanger trains will depend on the number of parallel trains.

For purposes of this Guideline, the following typical conditions were used for sample calculations:

1. A nominal size of 24-inch (61-cm) hot and cold headers assumed for a typical subfield.
2. A nominal size of 24-inch (61-cm) hot and cold headers assumed for the inlets and outlets of heat-exchanger (HX) trains.

3. For purposes of examining the flow condition and velocity profile in the headers, a nominal design velocity of 3 m/s (9.8 ft/s) is assumed.
4. The expected method for flow measurement is to measure the cold HTF side of the system at multiple locations to arrive at the total flow, either at the inlets of all the subfields, or at the outlet of the HX trains.

Table 5-1. Parameters Required for Determining Thermal Power Output and Efficiency of the Solar System

C – calculated M – measured P – physical property
 Pri – primary variable Sec – secondary variable

| Primary Term | Parameter | Typical Influence | Typical Source |
|---------------------|-----------------------------------|--------------------------|-----------------------|
| Solar Field Power | Energy out | Pri | C |
| | HTF mass flow | Pri | M |
| | HTF density | Pri | P |
| | HTF specific heat | Pri | P |
| | HTF temperature entering HX train | Pri | M |
| | HTF temperature leaving HX train | Pri | M |
| Solar Input | Energy in | Pri | C |
| | Solar resource: DNI | Pri | M |
| | Effective trough aperture area | Pri | P |
| | Solar time | Pri | M |
| | Latitude | Sec | P |
| | Longitude | Sec | P |
| | Solar field inclination | Sec | P |
| Other | Dry-bulb temperature | Sec | M |
| | Wet-bulb temperature | Sec | M |
| | Relative humidity | Sec | M |
| | Wind velocity | Sec | M |
| | Wind direction | Sec | M |
| | Mirror reflectivity | Pri | M |

5.3 Comments on Instruments and Measurements

It is not the purpose of this Guideline to provide a complete treatise on measurement methods, systems, or their accuracy. Rather, the user of this Guideline should review the general considerations on engineering measurements as applied to these acceptance tests based on a thorough study of ASME PTCs relevant to this application. However, specific information on specific types of instruments is provided below with regard to measuring devices required to measure the variables noted previously—particularly at the HTF flow conditions encountered in utility-scale trough systems and for solar-unique variables.

An instrument is a device for determining the value or magnitude of a quantity or variable. The variables of interest are identified above. Measurements may be direct or indirect. For example, measuring the temperature of the HTF with a thermocouple or resistance temperature detector (RTD) is a direct measurement. Measuring the flow rate of the HTF by use of a pitot tube or pressure drop across an orifice is an indirect measurement. Because of physical limitations of the measuring device and the system under study, practical measurements always have some error. The accuracy of an instrument is the closeness with which its reading approaches the true value of the variable being measured. Random error refers to the reproducibility of the measurement, that is, with a fixed value of a variable, how much successive readings differ from one another. Sensitivity is the ratio of the output signal or response of the instrument to a change in input of the measured variable. Resolution relates to the smallest change in measured value to which the instrument will respond.

Errors other than human error may be classified as systematic or random. Systematic errors are those due to assignable causes; these may be static or dynamic. Static errors are caused by limitations of the measuring device or the physical laws governing its behavior. Dynamic errors are caused by the instrument not responding fast enough to follow changes in the measured variable, e.g., lag in a temperature reading. Random errors are those due to causes that cannot be directly established because of random variations in the system.

There are several essential parts to an instrument measurement system, namely:

- Primary sensing element
- Transmitting means or system
- Output or indicating element
- Data storage system.

Considerable literature exists on the accuracy, installation, data acquisition, and data storage of measurement devices and systems, from both independent sources and from suppliers of the devices and data acquisition systems. The ASME has spent considerable effort to supply valuable recommendations on this subject (see appropriate PTCs, e.g., on flow and pressure measurement). The primary considerations are selection of the measurement device and system, calibration, and estimation of the systematic uncertainty. Random errors need to be estimated from repeated test runs or by analytical means.

5.4 Temperature Measurement

Resistance temperature detectors (RTDs) or thermocouples (TCs) are judged to be the most appropriate sensors to measure fluid temperature in the HTF stream. Table 4-2 summarizes the important characteristics of each for this application. Both are suitable, but as noted in the text below, the higher accuracy of the RTD suggests it is better suited for acceptance testing.

The RTD element can be made of different metals depending on the application, but platinum appears to be the most popular and is highly accurate. RTDs have a narrower operating range and a slower response time than thermocouples, but are potentially more accurate. For short-term performance testing purposes, accuracy is more important than durability (and ease of wire installation without affecting accuracy is desirable); these factors favor the choice of RTDs. Some RTDs can have significant drift during the break-in period, which must be considered. Their slower relative response than thermocouples is likely not an issue for performance testing but it needs to be considered if they are used in control loops. However, the lower relative durability of an RTD is a significant consideration if the device will be installed permanently. Also note that either sensor type can be integrated with the recommended flow instrument (e.g., Annubar or vortex meter).

Data measurement devices must be allowed to reach thermal equilibrium in the environment where the measurements will be taken. Thermocouple lead wires shall be placed in a nonparallel position relative to electrical sources to avoid possible electrical interference.

It is presumed, but not yet measured in practice, that the temperature is constant over the diameter of the header piping due to the fully mixed flow. At the end of each loop, the HTF is injected perpendicular to the header flow. In the long headers leading to the power-block area, there is a negligible or very low heat flux to ambient temperature through the pipe wall and insulation. The thermal boundary layer under this condition is very thin.

Table 5-2. Temperature Measurement Devices

| Sensor Type | Resistance Temperature Detector (RTD) Platinum 4-Wire | Thermocouple Type K |
|---|--|---|
| Accuracy for Temperature Range, ± °F | ~1.5°F (0.8°C) (DIN/IEC 60751 Class A, higher accuracy obtainable; e.g. 1/3 DIN or 1/10 DIN, if desired) [see Note 1 Refs] | ~2.5°F (1.4°C) |
| Suitable for 750°F | Yes | Yes |
| Insertion Requirement | Thermowell | Thermowell |
| Response Time | Decent (~30 s) | Good (depends on thermowell and thermocouple geometry, but generally better than RTD) |
| Stability | High | High |
| Repeatability | Very Good | Good |
| Drift | 0.1°–0.3°F (0.06°–0.17°C) per month (can be higher in break-in period) ¹ | 0.15°–0.4°F (0.08°–0.22°C) per month. ¹ May increase with cycling. |
| Linear | Very Good | Good |
| Covered by PTC 19.3 [see Note 2 Refs] | Yes | Yes |
| Durability/Life | Good (more reliable types can experience higher drift during first several months; then stable) | Better |
| Cost | Medium (industrial) to High (precision) | Low to Medium |
| Suitable | Yes | Yes |

Table 5-2 Notes

1) Primary element and the transmitter should be calibrated before and after the test in accordance with manufacture’s specifications to ensure that the expected accuracy is met. This exceeds the DIN/IEC 60751 requirement, and is intended to improve instrument accuracy.

2) References:

1. EPRI-TR-106453 “Temperature Sensor Evaluation” (6/1996)
2. ASME *PTC 19.3 - Temperature Measurement*
3. ASME *PTC 46 – Overall Plant Performance*
4. <http://www.omega.com/>

5.5 Flow Measurement

Accurately measuring the volumetric flow rate of the HTF is a significant engineering challenge, particularly in the large pipes that characterize utility-scale parabolic trough projects. ASME *PTC 19.5 – Flow Measurement* is the primary reference for flow measurements. ASME *PTC 6 - Steam Turbines* and ISO 5167¹³ provide further information on flow measurement techniques. These sources include design, construction, location, and installation of flow meters, connecting piping, and computations of flow rates. For the conditions of a solar system performance acceptance test, a number of flow measurement devices are suitable and have been evaluated on the basis of the most important criteria for this measurement. The results are given in Table 5-3. Usage in several plants has tended towards ultrasonic and vortex flow meters, but the choice for a specific project is up to the test parties. For good results, the Reynolds number in the measuring length should usually be turbulent, e.g., above 2300.

5.5.1 Velocity Profile¹⁴

If the flow measurement entails measuring velocity at discrete points across the pipe, the issue of the velocity profile is important. The following analysis provides insight on the velocity profile in a circular pipe with turbulent flow conditions for any fluid. At a peak velocity of 3 m/s in a 24-inch (61-cm) Schedule 40 header for the HTF at operating temperature, the Reynolds number is about $6.5 \cdot 10^6$, and it is fully established turbulent flow at that value. This fact sets the velocity profile based on fluid mechanics analysis and empirical data. The analysis starts with the knowledge that flow in a pipe is a bounded flow and is subject to no-slip boundary conditions on the walls and bounded by a limited region. But there is no established theory for pipe flow under a high Reynolds number. The only practical method to solve high-Reynolds pipe flow is using an empirical formulation derived from experimental data, which is called the log-overlap law. This formulation defines three layers for a pipe flow: an inner layer close to the wall, an outer layer close to the centerline, and an overlap layer between them. Laminar shear is dominant in the inner layer (<0.001% of radius) and turbulent shear dominates in the outer layer. The resulting flow profile for the example case stated above is shown in Figure 5-1.

¹³ ISO 5167 (International Organization for Standardization) Measurement of fluid flow by means of pressure differential devices inserted in circular cross-section conduits running full. Part 1: General principles and requirements; Part 2: Orifice plates; Part 3: Nozzles and Venturi nozzles; Part 4: Venturi tubes

¹⁴ Data provided by Dr. Guangdong Zhu of NREL.

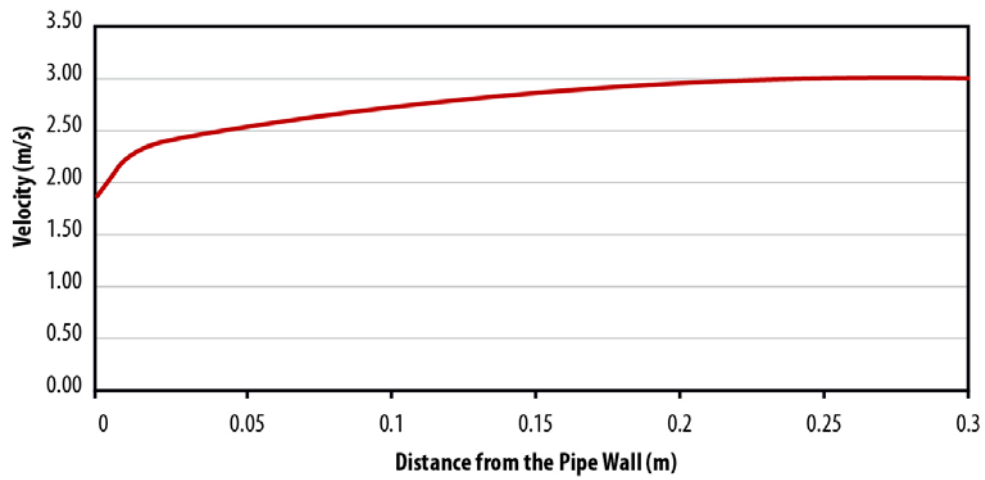


Figure 5-1. Fully developed velocity profile in a pipe. (Courtesy of NREL)

Table 5-3. HTF Flow Measurement Devices¹⁵

| ID | Instrument Type | Units | Differential Pressure Type | | | | Ultrasonic (Clamp-On) | Ultrasonic (Insert-Type) | Insertion Vortex | Insertion Turbine |
|----|---|----------------------|----------------------------|---------------------|---------------------------|-----------------|-----------------------|--------------------------|--------------------------|----------------------|
| | | | Orifice, Nozzle, & Venturi | V-Cone (McCrometer) | Averaging Port Pitot Tube | Segmented Wedge | | | | |
| 01 | Indicative Price Range | $\$/D^2$ (D=inch) | 46–220 (Venturi) | 62–170 | 8–90 | 57–80 | 18–225 | 33–139 | 4–47 | --- |
| 02 | Volumetric Accuracy | +/- % | ≤ 1.0–1.5 | ≤ 1.0 | 0.8–1.1 | 0.5 | 1.2 | ≤ 1.0 | 1.2 | 1.0–5.0 |
| 03 | Maximum Turndown Ratio | --- | 4:1 (and greater) | 10:1 | 7.5:1–14:1 | 8:1 | 30:1 | 15:1–150:1 | 7.5:1–15:1 | 15:1 |
| 04 | Permanent Pressure Drop | psi | 0.5–1 (Venturi) | 1–2 | < 0.1 | 2–4 | None | None | Minimal (avg pitot tube) | Minimal |
| 05 | “Vena-Contracta” Pressure Drop | psi | 4 (Venturi) | Unknown | 2–3 | 4–8 | None | None | Minimal | Minimal |
| 06 | Suitable for Operation at 600°F | Yes/No | Yes | Yes | Yes | Yes | Yes | Yes | Yes | Yes |
| 07 | Suitable for Operation at 750°F | Yes/No | Yes | Yes | Yes | ~Yes (735°F) | Yes | Yes | Yes | Yes |
| 08 | Calibration Requirements | --- | Moderate | Moderate | Significant | Moderate | Minimal | Minimal | Significant | Significant |
| 09 | Repeatability | % | 0.1 | 0.1 | 0.1 | 0.2 | 0.15 | 0.1–0.3 | 0.1 | 0.25 |
| 10 | Piping Requirements (Diameters Upstream, Downstream) | Dia. | 3–30U, 3–10D | 0–3U, 0–1D | 7–30U, 3–30D | 5–6U, 3–5D | 10–40U, 5–10D | 10U, 5D | 10–25U, 5D | 10–30U, 5D |
| 11 | Pipe Size Limitations | --- | All Sizes | All Sizes | One mnfr limited to ~24" | All Sizes | All Sizes | All Sizes | All Sizes | All Sizes |
| 12 | ASME MFC Specification | --- | 3M | --- | 12M | --- | 5M | 5M | 6M | 22 |
| 13 | Conclusion | --- | Suitable | Suitable | Suitable | Suitable | Suitable | Suitable | Suitable | Potentially Suitable |

¹⁵ The HTF flow meters used for acceptance testing and normal operation at the Andasol plants in Spain are permanently installed clamp-on ultrasonic flow meters. The meters were calibrated with water.

Table 5-3 Notes

General magnetic meters were not included because they will not work due to low HTF electrical conductivity. Coriolis meters were not included because of pipe size limitations. Insertion turbine meters are included, although accuracy is questionable. All meters are subject to severe inaccuracies if two-phase flow is present.

Units: Inches*2.54 = cm ; psi/14.5 = bar ; psi*6895 = Pa.

- 01 “D” is nominal pipe size in inches. In general, the lower end of the costs, in $\$/D^2$, are representative of 36” pipe; the higher costs are representative of 10” pipe. Note, a portion of the insert-type ultrasonic, V-Cone[®], segmented wedge, and Venturi meter costs include piping/components (i.e., pipe spool) that would otherwise be accounted for in the piping system costs where insertion or clamp-on devices are employed.
- 02 Accuracy is over turndown range. Most listed accuracies are for calibrated meters.
- 03 The turndown ratios listed are for a maximum pipe velocity of 15 ft/s.
- 05 The “Vena-Contracta” pressure drop is the local pressure drop, a portion of which is recoverable. Users are cautioned that flashing or cavitation may occur if inadequate line pressure is present, which can void flow measurement. With proper system design and operation, an adequate pressure margin above HTF vapor pressure should be obtainable.
- 08 Minimal = Internal diagnostics only; Moderate = Calibration of secondary transmitter equipment; Significant = “Moderate” plus periodic inspection of internal components. See “Instrument Notes” below for details on calibration and inspection for each instrument type.
- 10 Upstream and downstream straight length, expressed as pipe diameters, required for an accurate measurement. The upstream length requirement can be reduced with flow-straightening vanes.
- 13 It is not the intent to provide a recommended technology but rather to screen all flow measurement technologies and provide users with many feasible options and the pros/cons of each. See “Instrument Notes” below on Insertion Turbine. The orifice plate/flow nozzle/Venturi differential pressure types generally have low turndown capabilities and have significant pressure drop (with the exception of Venturi, as shown above) and will likely not be acceptable for measurement at low DNI and/or high incident angles (i.e., for reliability testing). The low turndown capability will be an issue on the steam/feedwater side as well, where these technologies have traditionally been used in performance testing.

Instrument Notes

Orifice/Nozzle/Venturi: Although these technologies are the most mature and are well accepted in ASME PTCs, turndown ratio and pressure drop limitations may preclude their use, with the exception of Venturi type. Within the Venturi family of meter types, low pressure drop options are available. Although these type of meters traditionally have accurate turndown ratios of 3:1 to 4:1, there are claims by certain manufacturers of 10:1⁺ with certain Venturi applications. Further investigation is warranted here. Periodic calibration of the external, secondary instruments (e.g., temperature, static P, delta P) is required.

V-Cone[®]: A V-Cone meter, manufactured by McCrometer, is a differential pressure device, measuring pressure before and after a conical insert, suspended in the center of the pipe. One of its main advantages is its nonprohibitive upstream and downstream piping requirements, although its pressure drop must be taken into account. Periodic calibration of the external, secondary instruments (e.g., temperature, static P, delta P) is required.

Averaging Port Pitot Tube: Kramer Junction Operating Company (KJOC) reported clogging and plating problems with this technology. After correspondence with Rosemount (the manufacturer of the Annubar), it was determined that an older, diamond-shaped model was originally used at the SEGS plants, whereas the current product offering is a “T” shape. There are other manufacturers of averaging port pitot tube devices, one of which claims to have a flow profile that is inherently less susceptible to plugging. Similar to the orifice/nozzle/Venturi, annual calibration of the secondary, external transmitters can be done while online. The internal devices need to be inspected periodically for fouling, which can be performed online (if appropriate “hot-tap” accessories are installed), although no measurement will be taken during inspection.

Segmented Wedge: The segmented wedge meter is a differential pressure device, somewhat similar to an eccentric Venturi meter, and has historically been used in slurry type applications where plugging or erosion can occur. Information in the table is representative of a remote seal connection type. Periodic calibration of the external, secondary instruments (e.g., temperature, static P, delta P) is required.

Ultrasonic: Many manufacturers are temperature limited, with only a few manufacturers capable of meeting the application’s temperature requirements and only one offering a clamp-on style that meets the temperature requirements and has reasonable accuracy. Ultrasonic (UT) meters are the mainstay in natural gas custody transfer applications that have high accuracy, reliability, and turndown requirements. UT meters have demonstrated, in other applications, as low as 0.15% accuracy at 15:1 turndown ratio and much higher turndown ratios at reduced accuracy. Note that the superior maintainability of UT meters described in the KJOC report ¹⁶Appendix R is due to the use of clamp-on type transducers; high accuracy UT meters are usually the insert type (e.g., wetted-transducer). Internal self-diagnostics can be performed on a UT transmitter while remaining online. Access to wetted transducers can only be obtained if fluid is evacuated from the meter section, which should be incorporated into the design (i.e., up/down stream isolation valves). The use of transducers (or more likely intervening materials due to high temperature) that are not flush with the pipe ID can theoretically erode (protruding type), or collect with sediment (cavity type), which can affect meter accuracy.

Insertion Vortex: Most manufacturers are temperature limited and KJOC Appendix R did report turndown issues. The internal devices need to be inspected periodically for fouling, which can be performed online (if appropriate “hot-tap” accessories are installed), though no measurement will be taken during inspection.

Insertion Turbine: Although published product literature theoretically would lend one to include an insertion turbine meter as an option (i.e., meets temperature, accuracy, and turndown requirements), the quote obtained for the specific application noted an accuracy range likely unacceptable for the testing purposes. There are inherent maintenance issues with moving parts, although the turbine can be inspected and/or repaired online with proper installation of “hot-tap” accessories.

¹⁶ Cohen, G.; Kearney, D.; Kolb, G. “Final Report on the O&M Improvement Program for CSP Plants,” Sandia National Lab Report SAND99-1290, June 1999.

5.5.2 Upstream/Downstream Requirements for Length/Diameter Ratio

For the instruments identified in Table 5-3, a certain amount of straight pipe upstream and downstream of the instrument is recommended to ensure a fully developed flow to achieve the expected accuracy of the instrument. The amount of downstream straight length pipe length/diameter ratio (L/D) is 4:5 for all devices. The amount of upstream straight pipe depends on the instrument and the fittings and or valves upstream of the instrument, but is generally at least 10 L/D of straight piping. For example, for a 24-inch (61-cm) header, an L/D=10 is about 20 ft (6 m) of straight pipe.

Flow conditioning devices can be located upstream of the instrument to reduce the recommended amount of straight length, but such conditioning will also introduce additional pressure drop.

5.6 Direct Normal Insolation

5.6.1 Components of Solar Radiation

Radiation can be transmitted, absorbed, or scattered by an intervening medium in varying amounts, depending on the wavelength. Complex interactions of the Earth's atmosphere with solar radiation result in three fundamental broadband components of interest to CSP technologies (see Figure 5-2). These components are:

- Direct normal insolation¹⁷ (DNI)—Solar radiation available from the solar disk
- Diffuse horizontal irradiance (DHI)—Scattered solar radiation
- Global horizontal irradiance (GHI)—Geometric sum of the component of DNI normal to a horizontal plane and DHI (total hemispheric irradiance).

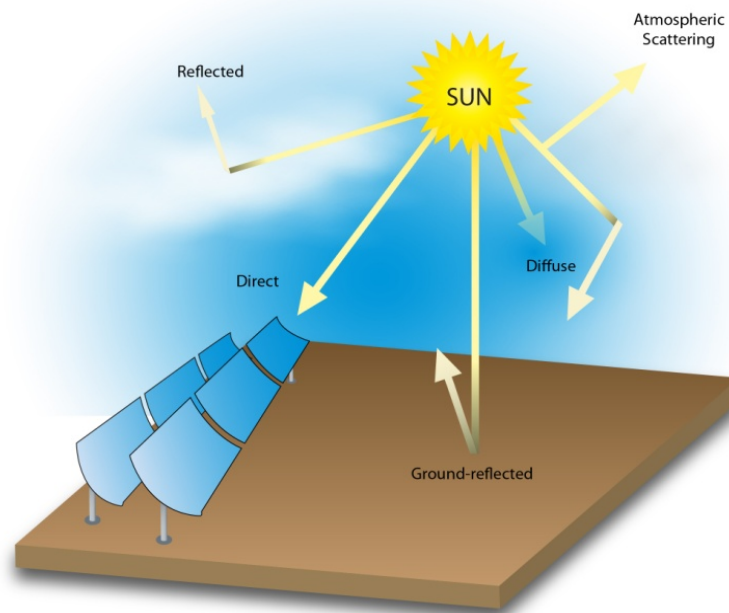


Figure 5-2. Components of solar radiation.
(Courtesy of NREL)

¹⁷ The terms “insolation” and “irradiance” are often used interchangeably.

A concentrating solar collector uses direct (or beam) radiation to redirect specular rays to the receiver.

5.6.2 Measurement Options

High accuracy is required for keeping the uncertainty low in the Acceptance Testing procedure. DNI is a very important input to the solar system performance model, and the heat input to the solar field is directly proportional to the DNI and the cosine of the angle of the sun’s rays to the aperture of the collector.

Two conventional devices—the rotating shadowband radiometer (RSR) and the 2-axis tracking pyrheliometer—are available to measure DNI, the first indirectly and the second directly. The pyrheliometer option is highly preferred for Acceptance Test purposes because of its accuracy, despite its cost.

The data in Table 5-4 are from the report, T. Stoffel, et. al, CSP: Best Practices Handbook for the Collection and Use of Solar Resource Data, NREL/TP-550-47465, Sept 2010.

Table 5-4. Estimated Direct Normal Sub-Hourly Measurement Uncertainties (Percent)

| Type A Error Source | U _{std} TP# | U _{std} Si [^] | Type B Error Source | U _{std} TP# | U _{std} Si [^] |
|---|-------------------------|-------------------------------------|---|-------------------------|-------------------------------------|
| “Fossilized” calibration error | 0.615 | 0.615 | “Fossilized” calibration error | 0.665 | 0.665 |
| Data logger precision (± 50 μV/10mV)* | 0.5 | 0.5 | Data logger precision (1.7 μV/10mV)* | 0.02 | 0.02 |
| Si detector cosine response | 0 | 0.5 | Si detector cosine response | 0 | 1.5 |
| Pyrheliometer detector temperature response (D20°C) | 0.25 | 0.05 | Detector temperature response | 0.25 | 0.05 |
| Pyrheliometer detector Linearity | 0.10 | 0.10 | Day-to-day temperature bias (10°C) | 0.125 | 0.10 |
| Solar alignment variations (tracker or shade band) and pyranometer level for Si | 0.2 | 0.1 | Solar alignment variations (tracker or shade band) and pyranometer level for Si | 0.125 | 0.10 |
| Pyrheliometer window spectral transmittance | 0.1 | 1.0 | Pyrheliometer window spectral transmittance | 0.5 | 1.0 |
| Optical cleanliness (blockage) | 0.2 | 0.1 | Optical cleanliness (blockage) | 0.25 | 0.1 |
| Electromagnetic interference and Electromagnetic field | 0.005 | 0.005 | Electromagnetic interference and electromagnetic field | 0.005 | 0.005 |
| TOTAL Type A** | 0.889 | 1.382 | TOTAL Type B** | 0.934 | 1.938 |

Thermopile detector used for a pyrheliometer.

[^] Silicon diode pyranometer detector used for an RSR.

* Typical manufacturer specified accuracy: ± 0.05% of full-scale range (typically 50 mV) -25° to 50 °C; assume 10 mV signal to ± 50 microvolts (μV)(0.5%) with 1.67 μV resolution (0.02%).

** Summed under quadrature.

As noted in the NREL report, the combined uncertainty can be determined from the standard uncertainties in the table for Type A and Type B errors for each detector type by summing in quadrature. The resulting standard uncertainty is 1.3% for a pyrheliometer option and 2.4% for an RSR option. The expanded uncertainty, representing a 95% confidence interval as described in Section 6 of these Guidelines, is 2.6% and 4.8% for the pyrheliometer and RSR, respectively.

Maintenance considerations—which are markedly simpler for the RSR device—figure into the choice of a unit for remote use, but are not important for the Acceptance Test application. Again, cost of the tracking pyrheliometer is high, but easily justified for this purpose.

For large solar fields (e.g., a 250-MWe trough plant may have 1.0 to 2.5 million square meters of aperture area and occupy a land area about three times larger), multiple DNI instruments are advised, although this is primarily a matter of judgment and agreement between the test parties. Under clear skies, the DNI should be uniform over areas of this size. For mental calibration, be advised that a single satellite measurement cell covers an area of about 10 km x 10 km, or 100 million square meters. Regarding solar field instrument placement, multiple instruments might be placed in discrete subsections of the solar field, which could translate to five or more instruments.

5.7 HTF Physical Properties

The properties of density and specific heat of the HTF are required to calculate the energy transferred out of the solar system into the heat-exchange train. The parties to the test must agree whether to accept the manufacturer's table of properties for a newly purchased fluid, or to have random samples tested. Samples will typically be sent to authorized laboratories. Test costs are expected to be on the order of several hundred dollars per sample per property. Representative samples of the HTF in the system during the performance test should be obtained using the methods described in ASTM D 4057 or ASTM D 5287. HTF oil should have a relatively consistent composition, similar to fuel oil. If HTF properties could vary because of outside factors, such as a changing source of HTF, a more rigorous sampling program will be required to ensure representative samples.

ASTM E-1269 is the standard typically used for specific heat measurements using digital scanning calorimetry (DSC). Multiple runs are required to reduce uncertainty in the measurements coming from a variety of contributors. It appears that the uncertainty in the specific-heat measurement can be on the order of $\pm 1\%$ to 3%, and it is not clear how much that property might vary over the large quantity of HTF in a solar field. It is also noted that HTF properties are typically measured at lower temperatures, and properties at the solar system operating temperature may differ somewhat at the higher temperatures.

The measurement of fluid density is more accurate, and one supplier states that the measured values are accurate well under 1%.

5.8 Mirror Reflectivity

Mirror reflectivity is an important input value to the solar system performance model. The primary instrument used at NREL and at operating plants is the D&S Portable Specular Reflectometer Model 15R-USB,¹⁸ designed for field and laboratory measurements of flat or

¹⁸ Information on this device is provided for information only and does not constitute a recommendation by NREL.

curved reflectors. According to the June 2009 NREL TroughNet site, the Model 15R has been extensively used at (all) the SEGS parabolic trough plants to measure mirror soiling for determining when mirror washing is required.

According to the manufacturer and reports from solar-field use, a single operator can take reflectance readings at the rate on the order of 3 to 4 per minute and record the readings to data sets stored in the instrument. Current detailed data from the operating plants is lacking. A USB port is provided for maintaining and downloading data sets and upgrading the firmware.

Uncertainty appears to be less than 1% with proper usage; human error in taking readings may be an important factor. A study performed by PSA (Spain) found the resulting uncertainty was less than 1% for a D&S 15R reflectometer, using 23 samples of back-silvered glass mirrors of different qualities and taking 228 measurements with different operators and ambient conditions.¹⁹

¹⁹ Personal communication with Eduardo Zarza, CIEMAT, September 2010.

6 Evaluation of Measurement Uncertainty

6.1 Measurement Uncertainty

Due to various influences, any test result will have an associated uncertainty. The uncertainty interval around a measured result describes our lack of knowledge about the true value of a measured quantity. Uncertainty can be reduced by many repeated measurements and in some instances can be further reduced through the use of redundant instruments.²⁰ The uncertainty of an interval about a measured value is usually expressed with a probability or level of confidence. Uncertainties arise from possibilities for error arising from or classified as: systematic errors, random errors, and human errors. It is very important in the measurements discussed here to quantify the uncertainty intervals to make judgments on the validity of the test results.²¹

Test uncertainty is an important element within any performance test code. ASME in particular has placed critical importance on test uncertainty analyses of all measurements and calculations associated with performance test codes. Therefore, significant attention has been paid to this aspect of the Guidelines. *ASME PTC 19.1 - Test Uncertainty* is devoted to this topic, and sections in some other codes address uncertainty analysis related to their respective topics.

Because of the resource variability and imperfections in control systems, variation in all of the measured parameters is inevitable. The frequency and period of data collection directly impacts the test uncertainty, and it is highly recommended that a pre-test uncertainty analysis be carried out prior to selection and subsequent installation of any instrumentation. An acceptance test will typically consist of more than one test run (data collected during a period of time in which the measured parameters are relatively steady). Conducting more than one test in addition to a post-test uncertainty analysis is recommended to verify the repeatability of the test results and the validity of the pre-test uncertainty analysis.

The systematic error associated with a measurement of a single parameter can come from many sources, including the calibration process, instrument systematic errors, transducer errors, and fixed errors of method. The test engineer should be diligent in identifying all of these sources of error, although it is often the case that one or several will dominate within a particular measurement parameter.

Random errors can similarly be based on a manufacturer's specification. However, the random uncertainty for a given measurement can be reduced based on repeated measurements over the interval in which the system is considered to be at steady state (defined by a minimal change in the ANI plus HTF flow control over the test period, such that the effects of thermal exchange between the HTF and solar field piping are negligible). For repeated measurements, the random standard uncertainty can be defined by

$$s_{\bar{x}} = S_x / \sqrt{N} \quad (\text{Eqn. 6-1})$$

²⁰ Redundant instruments are most readily used to reduce random errors associated with a measurement. To reduce systematic errors, the test engineer must calibrate the redundant instruments at different calibration laboratories to ensure that errors between the instruments are independent.

²¹In ASME PTCs, a great deal of attention is paid to uncertainty estimates. See, for example, *PTC 19-1 - Test Uncertainty* and *PTC 4-2008 - Fired Steam Generators*, Sec. 7.

where S_X is standard deviation of a series of sampled data and N is the number of data points collected over the test interval (e.g., 180 data points for a 30-minute test with data collected at 10-second intervals).

An example calculation is described below using the *PTC 19.1* principles and notation, and it is described in detail below.²² The purpose is to describe how the uncertainties in each of the measured variables X associated with an acceptance test propagate into the value of a calculated resulting quantity R .

Calculated results, such as the delivered power (Eqn. 3-1) and the solar thermal efficiency (Eqn. 3-2), are not typically measured directly, but rather, are based on parameters measured during the course of one or multiple acceptance tests. For this case, the result, R , is a function of individual or average values of these independent parameters as described by

$$R = f(\bar{X}_1, \bar{X}_2, \dots, \bar{X}_I) \quad (\text{Eqn. 6-2})$$

where the subscript i describes the number of parameters used in the calculation of the result and \bar{X} is either the value of a single measurement of the parameter or the average value of the parameter based on a number of N repeated measurements.

The expression for the combined standard measurement uncertainty of a calculated result based on multiple error sources can in many cases be calculated from the root-sum-square of the total uncertainty of the individual systematic and random error sources²³

$$u_R = [(b_R)^2 + (S_R)^2]^{1/2} \quad (\text{Eqn. 6-3})$$

where b_R is the systematic standard uncertainty of a result and S_R is the standard random uncertainty of a result as calculated by

$$b_R = \left[\sum_{i=1}^I \left(\frac{\partial R}{\partial \bar{X}_i} b_{\bar{X}_i} \right)^2 \right]^{1/2} \quad (\text{Eqn. 6-4})$$

$$S_R = \left[\sum_{i=1}^I \left(\frac{\partial R}{\partial \bar{X}_i} S_{\bar{X}_i} \right)^2 \right]^{1/2} \quad (\text{Eqn. 6-5})$$

²² Although this section is consistent with the methodology and notation used in *PTC 19.1*, the reader can additionally refer to “Measurement Uncertainty: Methods and Applications” by Ronald H. Dieck, ISA, Fourth Edition. This book describes the ASME methodology (among others) and uses consistent notation to the information presented in this Guideline.

²³ See ASME *PTC 19.1* or Dieck for exceptions to this case.

For the equations above, $b_{\bar{x}}$ is defined as the systematic standard uncertainty²⁴ of a component and $s_{\bar{x}}$ is the random standard uncertainty of the mean of N measurements. Definitions for the standard systematic and random uncertainty, as well as the methodology for calculating these values, are described in detail in *PTC 19.1* and Dieck.

The total standard measured uncertainty of the calculated result given by Eqn. 6-2 can be calculated using the methodology described above. It is important to note that this “standard” uncertainty implies that the calculated result will capture the true result within a 68% confidence level (one standard deviation). Typically, a confidence level of 95% (two standard deviations) is desired by the test engineer. For this case, the expanded uncertainty in the result is given by

$$U_{R,95} = 2u_R \quad (\text{Eqn. 6-6})$$

Example Calculation of Total Uncertainty for the Measurement of Solar Field Power

Applying Eqn. 6-4 to Eqn. 3-1 for the calculated solar field power, we get the following equation for the standard systematic uncertainty of the result²⁵:

$$\begin{aligned} b_R^2 &= \left(\frac{\partial R}{\partial m} b_m\right)^2 + \left(\frac{\partial R}{\partial C_p} b_{C_p}\right)^2 + \left(\frac{\partial R}{\partial T_{hxin}} b_{T_{hxin}}\right)^2 + \left(\frac{\partial R}{\partial T_{hxout}} b_{T_{hxout}}\right)^2 \\ &= \left(C_p(T_{hxin} - T_{hxout})\right)^2 b_m^2 + \left(m(T_{hxin} - T_{hxout})\right)^2 b_{C_p}^2 + (mC_p)^2 b_{T_{hxin}}^2 + \\ &\quad (mC_p)^2 b_{T_{hxout}}^2 \end{aligned} \quad (\text{Eqn. 6-7})$$

Similarly, Eqn. 6-5 can be used to derive the equation for the absolute standard random uncertainty of the result.

$$\begin{aligned} S_R^2 &= \left(C_p(T_{hxin} - T_{hxout})\right)^2 S_m^2 + \left(m(T_{hxin} - T_{hxout})\right)^2 S_{C_p}^2 + (mC_p)^2 S_{T_{hxin}}^2 + \\ &\quad (mC_p)^2 S_{T_{hxout}}^2 \end{aligned} \quad (\text{Eqn. 6-8})$$

²⁴ The test engineer should be careful in understanding what uncertainty may be represented by a manufacturer for a given measurement device. The standard uncertainty implies a 68% (one standard deviation) confidence level that the systematic error will fall within the uncertainty limits. The manufacturer may provide information that a 95% confidence (two standard deviations) level was chosen for the uncertainty. For this case, the test engineer should typically divide this value by 2 for use in this analysis. As a conservative estimate (for which the manufacturer does not state a confidence level), one should assume that the value provided is based on one standard deviation.

²⁵ In actual practice, volumetric flow would likely be measured in lieu of mass flow resulting in a revised equation for power, $P = \rho \sqrt{C_p} (T_{hx,in} - T_{hx,out})$, where both ρ and $\sqrt{C_p}$ are a function of the HTF temperature. A more detailed analysis of the uncertainties associated with the measurement of solar field power and efficiency would need to include these expanded terms.

Example Calculation of Total Uncertainty for the Measurement of Solar Field Efficiency

The above methodology can be applied identically to the equations for solar field efficiency to arrive at estimated uncertainties. The resulting equation for the standard systematic uncertainty associated with the solar field efficiency based on ANI is

$$\begin{aligned}
 b_R^2 = & \left(\frac{c_p}{DNI \cdot \cos\theta \cdot A_{aperture}} (T_{hxin} - T_{hxout}) \right)^2 b_m^2 + \\
 & \left(\frac{m}{DNI \cdot \cos\theta \cdot A_{aperture}} (T_{hxin} - T_{hxout}) \right)^2 b_{C_p}^2 + \left(\frac{m c_p}{DNI \cdot \cos\theta \cdot A_{aperture}} \right)^2 b_{T_{hxin}}^2 + \\
 & \left(\frac{m c_p}{DNI \cdot \cos\theta \cdot A_{aperture}} \right)^2 b_{T_{hxout}}^2 + \left(\frac{m c_p (T_{hxin} - T_{hxout})}{(DNI \cdot \cos\theta)^2 \cdot A_{aperture}} \right)^2 b_{DNI}^2 + \\
 & \left(\frac{m c_p (T_{hxin} - T_{hxout})}{(DNI \cdot \cos\theta \cdot A_{aperture})^2} \right)^2 b_{A_{aperture}}^2 \quad \text{(Eqn. 6-9)}
 \end{aligned}$$

and

$$\begin{aligned}
 S_R^2 = & \left(\frac{c_p}{DNI \cdot \cos\theta \cdot A_{aperture}} (T_{hxin} - T_{hxout}) \right)^2 S_m^2 + \\
 & \left(\frac{m}{DNI \cdot \cos\theta \cdot A_{aperture}} (T_{hxin} - T_{hxout}) \right)^2 S_{C_p}^2 + \left(\frac{m c_p}{DNI \cdot \cos\theta \cdot A_{aperture}} \right)^2 S_{T_{hxin}}^2 + \\
 & \left(\frac{m c_p}{DNI \cdot \cos\theta \cdot A_{aperture}} \right)^2 S_{T_{hxout}}^2 + \left(\frac{m c_p (T_{hxin} - T_{hxout})}{(DNI \cdot \cos\theta)^2 \cdot A_{aperture}} \right)^2 S_{DNI}^2 + \\
 & \left(\frac{m c_p (T_{hxin} - T_{hxout})}{(DNI \cdot \cos\theta \cdot A_{aperture})^2} \right)^2 S_{A_{aperture}}^2 \quad \text{(Eqn. 6-10)}
 \end{aligned}$$

Tables 6-1 through 6-4 summarize uncertainty data and results derived from the methodology described above as applied to the solar field power and efficiency calculations, and they can be considered an example of a pre-test uncertainty analysis. Although any such analysis must be undertaken with the specific system and instrumentation in mind, the systematic and random uncertainties of measurement parameters given in the tables represent what may occur in a typical field installation.²⁶

²⁶ Uncertainties within this Guideline are estimates based on discussions with various experts. Actual uncertainties will depend on specific solar field instrumentation and calibration procedures associated with an acceptance test.

Table 6-1. Table of Data – Solar Field Power

Independent Parameters

| Parameter Information (in Parameter Units) | | | | | | Uncertainty Contribution of Parameters to the Result (in Results Units Squared) | | | | |
|---|----------------------|---------|------------------|-----------------------|----------------|--|-------------------------|--|--|--|
| Symbol | Description | Units | Nominal Value | Standard Deviation | N _i | Absolute Systematic | Absolute Random | Absolute Sensitivity $\frac{\partial R}{\partial X_i}$ | Absolute Systematic | Absolute Random |
| | | | | | | Standard Uncertainty | Standard Uncertainty | | Standard Uncertainty Contribution | Standard Uncertainty Contribution |
| | | | | | | b_{X_i} | S_{X_i} | | $\left[\frac{\partial R}{\partial X_i} b_{X_i}\right]^2$ | $\left[\frac{\partial R}{\partial X_i} S_{X_i}\right]^2$ |
| m | Mass flow rate | kg/s | 1200 | 3.5 | 180 | 12 | 0.3 | 255.4 | 9395941 | 4567 |
| Cp | HTF specific heat | kJ/kg-K | 2.48 | .007 | 30 | 0.031 | 0.0013 | 1236000.0 | 14681159 | 24217 |
| Thxin | Hot HTF temperature | °C | 393 | 1.2 | 180 | 1.0 | 0.09 | 2976.0 | 8856576 | 71065 |
| Thxin | Cold HTF temperature | °C | 290 | 1.1 | 180 | 1.0 | 0.08 | 2976.0 | 8856576 | 59959 |

Table 6-2. Summary of Data – Solar Field Power

| Symbol | Description | Units | Calculated Value, R | Absolute Systematic Uncertainty, b _R | Absolute Random Standard Uncertainty, S _R | Combined Standard Uncertainty, u _R | Expanded Uncertainty of the Result, U _{R,95} | Expanded Uncertainty of the Result, U _{R,95} (%) |
|--------|-------------------|-------|---------------------|---|--|---|---|---|
| P | Solar Field Power | kJ/s | 306528 | 5894 | 400 | 5908 | 11816 | 3.9% |

Table 6-3. Table of Data – Solar Field Efficiency

Independent Parameters

| Parameter Information (in Parameter Units) | | | | | | Uncertainty Contribution of Parameters to the Result (in Results Units Squared) | | | | |
|---|--------------------------|--------------------|------------------|-----------------------|----------------|--|-------------------------|---|---|---|
| Symbol | Description | Units | Nominal Value | Standard Deviation | N _i | Absolute Systematic | Absolute Random | Absolute Sensitivity | Absolute Systematic | Absolute Random |
| | | | | | | Standard Uncertainty | Standard Uncertainty | | Standard Uncertainty Contribution | Standard Uncertainty Contribution |
| | | | | | | $b_{\bar{X}_i}$ | $S_{\bar{X}_i}$ | $\frac{\partial R}{\partial \bar{X}_i}$ | $\frac{\partial R}{\partial \bar{X}_i} b_{\bar{X}_i}^2$ | $\frac{\partial R}{\partial \bar{X}_i} S_{\bar{X}_i}^2$ |
| m | Mass flow rate | kg/s | 1200 | 3.5 | 180 | 12 | 0.3 | 0.0006 | 0.000057 | 0.0000000 |
| Cp | HTF specific heat | kJ/kg-K | 2.48 | 0.007 | 30 | 0.031 | 0.0013 | 0.3040 | 0.000089 | 0.0000001 |
| Thxin | Hot HTF temperature | °C | 393 | 1.2 | 180 | 1.0 | 0.09 | 0.0073 | 0.000054 | 0.0000004 |
| Thxin | Cold HTF temperature | °C | 290 | 1.1 | 180 | 1.0 | 0.08 | 0.0073 | 0.000054 | 0.0000004 |
| DNI | Direct Normal Insolation | J/s-m ² | 950 | 11.2 | 180 | 12.5 | 0.8 | 0.8 | 0.000098 | 0.0000004 |
| A _{Aperture} | Collector Aperture SM=1 | m ² | 425000 | -- | -- | -- | -- | -- | -- | -- |

Table 6-4. Summary of Data – Solar Field Efficiency

| Symbol | Description | Units | Calculated Value, R | Absolute Systematic Standard Uncertainty, b _R | Absolute Random Standard Uncertainty, S _R | Combined Standard Uncertainty, u _R | Expanded Uncertainty of the Result, U _{R,95} | Expanded Uncertainty of the Result, U _{R,95} (%) |
|--------|------------------------|-------|---------------------|--|--|---|---|---|
| η | Solar Field Efficiency | -- | 0.754 | 0.018 | 0.001 | 0.018 | 0.035 | 4.7% |

7 Comments on Test Procedures and Plan

The test plan needs to be organized and developed according to the specific solar system design and to carefully consider both the previous discussion and ASME test code information to arrive at uncertainty results that are agreed upon by the test parties. For example, ASME *PTC 4-2008 – Fired Steam Generator* gives excellent guidance on preparations and guidance of performance testing. That code recommends that the preparation for testing include:

- Indisputable records on the equipment, test procedure, instrumentation characteristics locations, and calibrations
- Agreements on a wide number of issues that might later lead to misunderstandings
- Preliminary test runs to check out all aspects of the performance acceptance test procedures and data reduction
- Issues related to the conduct of the tests, e.g., preparation, starting and stopping, and readjustment of equipment or instruments during the test run periods
- Conduct of test and data collection.

Further recommendations cover instruments, operating conditions, and records.

7.1 Test Plan

The Test Plan in the example organization scenario of these Guidelines would be prepared by the EPC contractor, with comments by the technology provider and likely an independent engineer(s) representing the owner and debt providers. The plan translates guiding principles into a detailed program related to the specifics of the solar system being tested, based on the contractual agreements between the test parties. It is crucially important to cover all aspects of the testing and to document all agreements and methods. Instrumentation would typically be identified by instrument type and measurement, with location later verified visually in the field. More instrument details, such as serial numbers and calibration information, would be provided as they become available. Testing plans should be spelled out in detail as to purpose, duration, methods, data reduction, and pass/fail criteria. Test reports should be complete, with ample use of photographs and diagrams. For further information, see: *PTC 4-2008 – Fired Steam Generator*; *PTC 46 – Overall Plant Performance*; *PTC 50 - Performance Test Code for Fuel Cell Power Systems Performance*; and *PTC 19.1 - Test Uncertainty*.

To be clear, an independent Test Plan document must be written, based on these Guidelines and/or applicable ASME test codes, defining details of the performance acceptance testing. That document will become part of the contractual agreement between the party turning over the solar system and the party taking control of the solar system. Said differently, the Test Plan is a commercial agreement that will dictate the required testing for the transaction. The following bullet points and example outline in Section 7.1.3 are provided to show some elements of the use of the Guidelines in both the contract agreements and the test plan itself. In a general sense, the Guidelines (and eventually, an ASME PTC) provide the technical basis to produce a Test Plan that is specific to the project configuration, selected instrumentation, and other elements particular to the solar system under test.

7.1.1 Example of Contract Agreements Prior to Formulation of a Test Plan²⁷

- Total plant electrical performance guarantees are agreed to prior to signing of the EPC contract. Typically, only one or at most two system load points are guaranteed, usually at design capacity or near design capacity. Subsystem guarantees would typically be set at that time. Guarantees and requirements for the solar system may vary considerably between projects, EPC firms, and the solar system technology provider.
- To provide a wrap-around warranty, the usual EPC practice is to get back-to-back performance guarantees from major equipment suppliers. It is common to strive to pass through major equipment supplier terms, conditions, and exceptions to the contract.
- The performance test procedure is not developed prior to contract signing; however, the contract language typically includes "mutually agreed performance test procedure to be developed and approved by owner ~6 months prior to testing." The contract will also include major test-related principles so that no surprises occur when the test procedure is issued. Test procedures typically follow the appropriate ASME PTC, including sample calculations, correction curves (if any), and sometimes a calculation spreadsheet.
- A contract typically requires demonstration of values less than the guarantees (perhaps by 5%) prior to retirement of scheduled liquidated damages (substantial completion). This is known as "Minimum performance or minimum performance levels." Achievement of guarantees (or better) is to be performed prior to Final Completion. The duration typically allowed for Substantial Completion to Final Completion is about 6 months to 1 year.
- Contracts typically allow payment of performance-liquidated damages in lieu of achieving guarantee values, provided "minimum performance" criteria are achieved.

7.1.2 Some Elements of a Test Plan

- The guarantee values typically are included in the prime contract. Test specifics are usually covered in an Exhibit to the prime contract.
- The contract defines any commercial tolerance (which may or may not be linked to test uncertainty) allowed for pass/fail criteria.
- Contract-defined tests are to follow appropriate ASME PTCs as possible. Because the ASME PTC on CSP systems (PTC 52) is currently under development and appears to be several years away from the issue date of these Guidelines, we recommend that these Guidelines and ASME PTCs such as those on uncertainty and instrumentation be among the sources used to formulate the Test Plan.
- Both the EPC contractor and Owner nominate a person authorized to approve variations in test procedures, equipment/valve line-up, etc.
- The Owner typically has an Owners Engineer or third-party testing contractor acting on their behalf.

²⁷ Comments on these two pages extracted from personal communication with Marcus Weber, Fluor, December 2009, and David Ugolini, Bechtel Power Corp., July 2010.

- In practice, it is recommended that over test periods of several hours, or even days, per agreement between parties, data be taken continuously via the data acquisition system and processed in a post-test period through data reduction software. These data will not only document the Energy Test results, but will also serve to determine whether valid test run periods of 15 to 30 minutes can be identified in the Power Test. If desired, the data could be examined in real time using the same techniques to monitor progress through the test period.
- Preliminary test results/reports are typically required soon after test completion. The final test report is due later and includes laboratory analysis of fuel samples, test data, operator logs, and calculations. (A typical example list is in ASME *PTC 46 – Overall Plant Performance*.)

7.1.3 Sample Test Report Outline²⁸

1. Scope and Objective
2. Definitions
3. Testing Methodology
 - Measured Parameters
 - Modeled Parameters
 - System Operation
 - Equipment in Service
 - DCS and Manual Data Collection
 - Description of Performance Model
 - Data Processing and Model Run
 - Responsibilities of Parties
4. Testing Procedure
 - Pre-test Plant Condition
 - Operation prior to Data Collection
 - Operation during Testing
 - Operation after Testing
5. Data Collection and Analysis
 - Calculation Procedures
 - Correction Factors
 - Uncertainty
 - Data and Results Distribution

²⁸ Based on input from M. Weber, Fluor and M. Henderson, and R.W. Beck

- Acceptance Criteria
6. Appendices
- Valve Positions
 - Instrument Data Points
 - Test Results
 - Performance Analysis
 - Representative Model Input/Output
 - HTF Thermal Properties
 - Sample Calculation

7.2 Further Observations

7.2.1 General

In principle, the fundamental measured parameters and guiding equations for this Acceptance Test are straightforward, as shown in Section 3. The data required and computational methods for determining the performance of utility-scale solar thermal systems have been discussed in some detail in the previous sections, including data acquisition principles, instruments, and methods of measurement. Nevertheless, it is important to emphasize that there are many important considerations that must be addressed to ensure high-quality results. For this Acceptance Test, we reiterate a few important factors:

- Thermal equilibrium and stabilized conditions in the test runs for solar thermal power output and efficiency
- Acceptable measurement techniques for temperature, volumetric flow rate, and DNI, with all calibrations current
- Accurate HTF property values that are accepted by the principal parties involved in the testing
- Suitable locations for test measurements to ensure accurate results for a large solar system
- Acceptable uncertainty analyses throughout the test(s), with predetermination of systematic and random uncertainties
- Complete test logs and records of test data and data reduction methods
- Preliminary (practice) test runs to identify any problems or inconsistencies
- Pre-agreed-upon methods to deal with test anomalies and inconsistencies during testing.

Relevant ASME performance test codes contain excellent, more detailed information about best practices for conducting performance acceptance tests. For example, they provide good guidance on measurement data reduction, including calibration corrections, handling test-point outliers, methods of averaging data, if required, and computations of random and systematic uncertainty. *PTC 46 – Overall Plant Performance* and *PTC 4-2008 – Fired Steam Generators* offer good

examples. Complete records of test data and data reduction methods are critical. All instrument calibrations should be current.

7.2.2 Summary of Agreements To Be Made Between Test Parties

The following list summarizes the various topics noted in these Guidelines that must be agreed to by the Test Parties:

- Complete procedures and Test Plan for performance acceptance tests
 - Structure of tests (see below)
 - Selection and placement of flow and temperature instrumentation at solar subfields and at HX trains
 - Pass/fail criteria for evaluation of test results
 - Schedule of mirror washing during tests, pattern of reflectivity measurements, and basis for soiling factor to be used in performance model
 - Test schedule(s)
 - Requirements for demonstration of rated solar thermal design power capacity and rated solar thermal design efficiency
 - Selection of ANI or DNI as basis for efficiency measurement
 - Method of comparison between measured performance and model projected performance, and method of incorporation, or not, of test uncertainties into this comparison
 - Decision on measurements.
 - HTF properties (density; specific heat)
 - Multiple DNI locations
 - Single sensor or array of sensors at pipe measurement locations for flow and temperature measurements.
- Solar System performance model
 - Model selection (recommend model used for commercial *pro forma* performance projections)
 - Input data set to model (both fixed and per test values).
- Structure of short duration steady-state Thermal Power Test
 - Steady-state test run duration
 - Repeated number of steady-state tests per day, number of test days, and duration of multi-day steady-state test period
 - Criteria that would cause a temporary interruption in the agreed-upon test period.
- Structure of multi-day Continuous Energy Test
 - Duration of test period.
- Uncertainty analysis

- Random and systematic uncertainties for each parameter
- Exact equations and methods to be used
- Pre-test uncertainty analysis
- Data collection
- Post-test analyses.
- Test report
 - Complete details and table of contents of test report
 - Data reduction procedures and equations
 - Schedule for completion.